



LUND UNIVERSITY

Spatial Xenon Instability in Thermal Reactors

Olsson, Gustaf

1969

Document Version:

Publisher's PDF, also known as Version of record

[Link to publication](#)

Citation for published version (APA):

Olsson, G. (1969). *Spatial Xenon Instability in Thermal Reactors*. (Technical Reports TFRT-7005). Department of Automatic Control, Lund Institute of Technology (LTH).

Total number of authors:

1

General rights

Unless other specific re-use rights are stated the following general rights apply:

Copyright and moral rights for the publications made accessible in the public portal are retained by the authors and/or other copyright owners and it is a condition of accessing publications that users recognise and abide by the legal requirements associated with these rights.

- Users may download and print one copy of any publication from the public portal for the purpose of private study or research.
- You may not further distribute the material or use it for any profit-making activity or commercial gain
- You may freely distribute the URL identifying the publication in the public portal

Read more about Creative commons licenses: <https://creativecommons.org/licenses/>

Take down policy

If you believe that this document breaches copyright please contact us providing details, and we will remove access to the work immediately and investigate your claim.

LUND UNIVERSITY

PO Box 117
221 00 Lund
+46 46-222 00 00

SPATIAL XENON INSTABILITY IN THERMAL
REACTORS

GUSTAF OLSSON

REPORT 6910 JULY 1969
LUND INSTITUTE OF TECHNOLOGY
DIVISION OF AUTOMATIC CONTROL

SPATIAL XENON INSTABILITY IN THERMAL REACTORS

Gustaf Olsson

ABSTRACT

Xenon spatial oscillations in cylindrical thermal water reactors have been analysed with several different models. The fundamentals of the problem are discussed and different mathematical models are described.

The nature of the oscillations makes it possible to approximate the axis of the reactor core with only two points. This two point model gives a good physical insight in the problem and is shown to be rather accurate.

The linearized two point model can be treated analytically, and the influence of different parameters are compared with more complex models. The partial differential equation has also been approximated by several meshpoints in space. Calculations show how the critical values of the parameters vary with the number of meshpoints.

The nonlinear two point model has predicted unstable and stable periodic solutions, which have been verified by simulation of a more complex nonlinear model.

If a control rod is used to maintain criticality it is shown, that the rod does not affect linear stability in some cases. The nonlinear behaviour is, however, very much influenced by the rod. The temperature feedback has also a big influence on linear stability as well as nonlinear behaviour.

TABLE OF CONTENTS	Page
1. INTRODUCTION	1
1.1 The xenon oscillation problem	1
1.2 History of the problem	2
1.3 Summary of the results	3
2. MATHEMATICAL MODELS	5
Introduction	5
2.1 Approximations	7
2.1.1 The axial problem	7
2.1.2 Assumptions about the core	7
2.2 Fundamental equations	8
2.2.1 Neutron equation	8
2.2.2 Xenon and iodine equations	9
2.2.3 Boundary conditions	9
2.2.4 Incremental equations	10
2.2.5 Finite differences	11
2.3 Behaviour of the solution	12
2.4 Different mathematical models used by other authors	14
2.4.1 Linear modal expansion models	14
2.4.2 Nonlinear space independent models	15
2.4.3 Digital and analog simulations	16
2.5 A nonlinear spatial difference axial model, the TRAXEN model	16
2.6 A two space point axial nonlinear model	17
2.6.1 System equations	18
2.6.2 Neutron flux equations at different control types and symmetric equilibrium flux	21
2.7 A linearized two space point model	22
2.7.1 Linearization of system equations	23
2.7.2 The linearized neutron flux equation and the system equations for asymmetric flux	23
2.7.3 The linearized system equations for symmetric flux	25
2.8 A linear space difference multipoint model	27
2.8.1 General system equations	27
2.8.2 Special case I: flat equilibrium flux	28
2.8.3 Special case II: sinusoidal equilibrium flux	34

	Page
3. PHYSICAL AND TECHNOLOGICAL CONSIDERATIONS	36
3.1 Criterion of stability. Practical stability	36
3.2 Choice of reactor core parameters	37
3.3 Typical disturbances	38
4. LINEAR STABILITY ANALYSIS	39
4.1 The two point flux model stability	40
4.1.1 Influence of core parameters	40
4.1.2 Influence of asymmetry of flux	46
4.2 Influence of the number of meshpoints on stability calculations	47
4.2.1 Critical core height	47
4.2.2 The eigenvalues for some different numbers of node points	49
4.3 Comparison between different models of influence of certain core parameters	53
4.3.1 Dependence of mean flux level	53
4.3.2 Dependence of temperature coefficient	54
4.3.3 Flux form influence	55
5. CHARACTER OF THE SOLUTIONS OF THE NONLINEAR MODELS	57
5.1 The two point model	57
5.1.1 Qualitative discussion of influence of nonlinear terms	57
5.1.2 Periodic solutions with rod control	58
5.1.3 Periodic solutions with homogeneous control	64
5.2 Comparisons between the two point model and the non-linear transient studies with TRAXEN	67
5.2.1 Rod control	67
5.2.2 Homogeneous control	69
REFERENCES	71
APPENDIX 1	
1	Definition of symbols and their numerical values
2	Program listings

1. INTRODUCTION

1.1 THE XENON OSCILLATION PROBLEM

In large power reactors there is a problem of spatial stability depending on such parameters as size, flux level and spectrum, fission yields, temperature feedbacks and core geometry.

Xenon-135 is the fission product which is the most important for spatial oscillations because of its very large thermal cross section ($\sim 2.8 * 10^6$ barns) for neutrons. In thermal reactors the effect on reactivity is so big, that xenon has been known and allowed for in reactor design since it was first detected through an unexpected loss of reactivity in the first Hanford reactors [1]. Typically, Xe-135 is responsible for a 2 to 3% loss in reactivity following a few hours of full power operation.

There are two different problems, which are caused by xenon. It causes large reactivity transients in the core when the total power is altered. This problem is not treated in this report. Moreover, divergent oscillations of the spatial flux distribution are possible in large reactors due to xenon, see figure 1. These oscillations will cause hot spots of the power, which must be avoided.

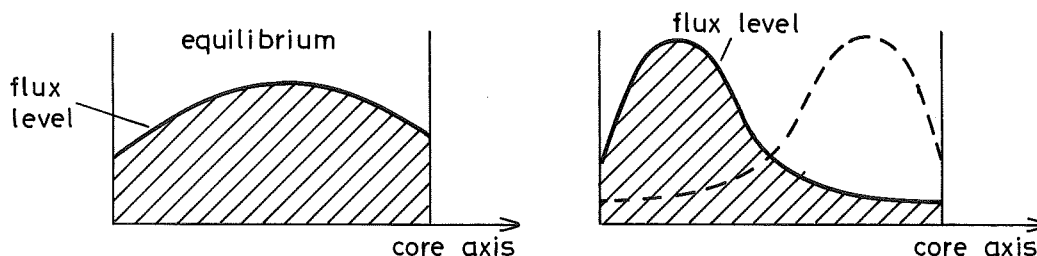


Fig. 1. Hot spots in flux distribution.

The xenon stability problem is thus a distributed problem.

The fundamental equations are a nonlinear partial differential equation coupled to nonlinear ordinary differential equations.

The aim of this report is to study the one-dimensional axial xenon stability, first by means of a crude dynamical model. This model is used in order to see how different core parameters and nonlinearities influence the reactor stability. Then the model is compared to refined models by means of analysis and digital simulation. Digital simulations of a nonlinear axial core model are described in [15].

1.2 HISTORY OF THE PROBLEM

The xenon spatial stability problem was first demonstrated in Savannah River [4], where an axial flux oscillation appeared in December, 1955. The oscillation proceeded for 14 days, while the power was constant. The period was found to be 28 hours. In Shippingport [11],[19] an oscillation of 3-5% with a period of 24 hours was observed at the first fuel charge. Xenon oscillations were found in the second fuel charge also.

The first analysis of the xenon oscillations appeared in 1956. Ward [23] described the problem and made a stability analysis. The analysis was continued and extended by Henry and Germann 1957 [5] and Randall and St. John 1958 [17].

After 1958 a great number of theoretical and experimental studies have been made. Most of the papers are based on linearized equations. As all power reactors had to be built inherent stable for xenon, all the papers treated the problem to describe the appearance of the oscillations in terms of stability criteria.

In general, the conditions for oscillations to occur are large core size and high flux level, which now are within the range of the specifications of modern power reactors.

A great number of references is found in Wiberg [24]. An excellent summary of progress through 1964 has been given in the Geneva Conference paper of Kaplan et al [8]. Additional analytical and simulation studies are presented [7-10], [13], [14], [16], [21], and some experimental verifications are presented in [6].

Non-linear analysis was made first by Chernick [1]. Later Lyapunov's method has been used in some papers for space independent reactor models [3], [18], [20].

Wiberg [24] and Stacey [22] have used modern control theory for a reactor in which spatial kinetic effects are important.

More details about the models are presented in section 2.4.

1.3 SUMMARY OF THE RESULTS

The xenon oscillations may appear in all three spatial dimensions, but this report deals only with the axial problem. In chapter 2.1 is discussed the reasons why the axial problem is important.

The dynamical behaviour is described by a nonlinear partial differential equation coupled to nonlinear ordinary differential equations. The general behaviour of the solution is discussed in 2.3. Because of the complexity of the equations several authors have made different approximations to get suitable models. In 2.4 and 2.5 are presented the most common models. The linearized ones are either based on eigenfunction expansions or difference approximation. Nonlinear models are derived either from space independent reactor dynamics or from difference approximation of the core.

A big part of this work is based on a nonlinear two space point reactor model, described in 2.6. The neutron diffusion equation is given only in two points along the core axis. The model is linearized in 2.7. The linear model is generalized to several space points in 2.8.

It is shown in 2.7 that the Lyapunov - Poincaré theorem is valid for the two point model, why stability can be determined with the linear equations.

As criticality must be maintained by a control rod or by homogeneous absorption in the core it is interesting to know how stability is affected by this absorption. It is shown in 2.7 and 2.8 that critical height is independent of absorption configuration for symmetric fluxes in the two point model and for flat fluxes in the model with many space points.

Chapter 3 presents practical considerations of xenon instability. The choice of core parameters is discussed in 3.2. As the dynamical behaviour is nonlinear the disturbances are important and in 3.3 is discussed typical disturbances.

The linear two point model is easy to handle analytically. In 4.1 is discussed influence of different core parameters on stability. The model has been very useful to detect relationships between parameters. Thus was found an interesting relationship between critical core height and mean flux level.

The two point model is compared to more complex models with good agreement in 4.2 and 4.3.

The critical height for different flux shapes is calculated for different models with different number of finite differences of the core axis.

It is shown for flat flux and sinusoidal flux, that the critical height as function of the number of node points converges asymptotically towards a finite value when complexity (number of space points) increases.

Out of a calculation of critical core height with 2, 3 and 4 meshpoints, the asymptotic value is extrapolated within 3%. The period of oscillation at critical height and dependence of temperature coefficient are approximated accurately for flat flux with a two point model.

Even in the nonlinear case, the two point model has been useful to predict interesting features of the xenon trajectories. In chapter 5 is discussed the influence of nonlinear terms on xenon instability. The two most important terms are the temperature feedback and the neutron absorption (control) term. These terms will decide if periodic solutions will appear for a certain flux form and core height. Both unstable and stable periodic solutions can appear. This type of oscillations are verified by digital simulation of a more complex nonlinear model. There are quantitative differences of amplitudes between the models. They are explained and discussed in 5.2.

2. MATHEMATICAL MODELS

INTRODUCTION

In this chapter are some common linear and nonlinear models described, which have been used to solve the xenon stability problem.

In order to simplify the study, we list the names of the models at first. All the space models are one-dimensional. We call them axial models as they describe the axial flux distribution.

- Linear modal expansion models
- Space independent models
- The TRAXEN model. A nonlinear finite difference model with
 - a) rod control
 - b) homogeneous control.
- Two space points model, which is
 - nonlinear or linear,
 - symmetric or asymmetric,
 - and have
 - flat flux or sinusoidal flux in equilibrium
 - rod control or homogeneous control.
- Linear multipoint model. A finite difference model with variable number of space points.

In section 2.1 is presented the reasons why we have treated the axial problem. The simplifications of the model are also listed.

The fundamental equations which describe the dynamics are described in 2.2. They are the neutron balance equation, a diffusion equation, and two ordinary differential equations. These two equations describe the change of xenon and iodine respectively. They are called

- a) xenon equation and
- b) iodine equation

later in this report.

The neutron equation is approximated by finite space differences and is assumed to be stationary. This makes it to a finite number of algebraic conditions.

The behaviour in general of the solution is discussed in 2.3.

The rest of the chapter describes a number of xenon models.

In 2.4 is described the linear modal expansion models. There is only one complete eigenfunction expansion of the state equations, the Kaplan modes. Due to numerical difficulties, however, even other modes have been used, and the most common ones are the clean reactor modes.

Some simple nonlinear space independent models have been used to show the existence of periodic solutions.

The TRAXEN nonlinear finite difference model is described in 2.5. It has been used in digital simulations, which are reported in [15]. TRAXEN has also been used to compare the results from the two point model.

The two point model is derived in 2.6. In the nonlinear case it is only derived for symmetric equilibrium flux. By rod control in this model we mean, that absorption is only varied in one space point to maintain criticality, while the other space point has constant absorption. At homogeneous control both space points have the same absorption.

The linearized two space point model, in 2.7, is a linear fourth order system. It is shown that Lyapunov - Poincaré theorem is valid for the two-point model. It is also proved that stability is independent of control type in the symmetric flux case.

A multipoint model is derived in 2.8. Even for this model it is shown that stability is independent of control type, provided the flux is flat in equilibrium. Two special cases are treated, the flat and the sine flux. We define a sine flux to have equal buckling in every space point. The flux shape converges to a real sine curve when the number of space points grows to infinity.

2.1 APPROXIMATIONS

2.1.1 THE AXIAL PROBLEM

In this report is only studied the axial xenon stability problem. This is done of following reasons:

- It is suitable to build water moderated reactors in cylindrical tanks. Technological reasons make it preferable to increase height rather than diameter, which causes the xenon problem to be serious in axial direction.
- The cooling channels are oriented axially, which causes the void in a boiling water reactor to affect the xenon axial stability. Thus the diffusion is space dependent. This problem, however, has not been studied here, even if programs [15] has been prepared for hydrodynamic studies.
- It is important to study the influence of control rods on xenon stability. The movement may be rather big. This will affect the amplitude and the stability of the oscillations very much. Moreover, an oscillation can be introduced by a rod during the start-up of the reactor or at refuelling.
- Depending on control rod configuration axial oscillations are more difficult to control than azimuthal or radial oscillations.
- Security reasons make it necessary to build the reactors inherent stable for axial xenon oscillations.

2.1.2 ASSUMPTIONS ABOUT THE CORE

We have assumed the following simplifications in the models:

- the variables are separable in space and time,
- top and bottom reflectors are neglected, and the thermal flux is zero on the core boundary,
- fuel elements and control rods will reach the whole area between the extrapolated boundaries,
- power production in moderator and fuel have been combined,
- the power control system is always stable (only prescribed variations of the total power can appear).

- the temperature effects on buckling are proportional to flux variations,
- only one control rod (the absorption in the rod is assumed to be constant),
- diffusion theory is assumed even near the rod boundary,
- only the absorption cross section is affected by the control rod,
- the microscopic cross section of xenon is independent of temperature in the actual temperature range,
- no stochastic disturbances are treated.

2.2. FUNDAMENTAL EQUATIONS

2.2.1 THE NEUTRON EQUATION

The neutron balance is described by the Boltzmann equation in the general case. This equation may be adequately approximated by multigroup diffusion equations.

Since the xenon oscillations are expected to occur only in large thermal reactors, the distribution of the thermal neutron flux is treated by one-group diffusion theory.

As the xenon oscillations are very slow compared to neutron life time, we assume that the neutron flux is stationary in every moment.

We also neglect the influence of delayed neutrons. The diffusion equation then reads:

$$\nabla \cdot (D \cdot \nabla \phi) + (\nu \Sigma_f - \Sigma_a) \phi = 0$$

where $\phi(r, t)$ is the neutron flux.

We divide the equation with a suitable mean value of the diffusion constant D^0 and get the equation:

$$\nabla(E \cdot \nabla \phi) + B^2 \cdot \phi = 0 \tag{1}$$

$B^2(r, t)$ is the space and time dependent material buckling of the poisoned reactor. The buckling primarily determines the flux. E is the normalized diffusion constant.

2.2.2 XENON AND IODINE EQUATIONS

The fundamental equations for xenon and iodine process in nuclear reactors can be found elsewhere [2]. They are by convenience repeated here:

$\frac{\partial X}{\partial t} = -\lambda_X X + \lambda_I I + \gamma_X \sigma_X \phi - \sigma_X X \cdot \phi$	(2)
$\frac{\partial I}{\partial t} = -\lambda_I I + \gamma_I \sigma_X \phi$	(3)

where $X = X(x, t)$ and $I = I(x, t)$ are functions of space and time.

They are normalized to the saturation value of xenon for infinite flux.

All symbols are explained in Appendix 1.

2.2.3 BOUNDARY CONDITIONS

The initial conditions are determined by the equilibrium values of neutron flux, xenon and iodine (1) - (3). Furthermore, the flux is zero on the extrapolated boundary of the core axis.

$$\phi(0, t) = \phi(H, t) = 0 \tag{4}$$

This implies directly

$$\begin{aligned} X(0, t) = X(H, t) &= 0 \\ I(0, t) = I(H, t) &= 0 \end{aligned} \tag{5}$$

The power condition reads:

$$\int_z K(z) \cdot \phi(z, t) dz = P(t) \tag{6}$$

where $K(z)$ is a weight function and $P(t)$ is total power.

2.2.4 INCREMENTAL EQUATIONS

It is convenient to write the equations in incremental form. Let us assign

$$\begin{aligned}\phi(z,t) &= \phi^0(z) + \varphi(z,t) \\ X(z,t) &= X^0(z) + \xi(z,t) \\ I(z,t) &= I^0(z) + \eta(z,t)\end{aligned}\tag{7}$$

where the superscripts mean equilibrium values.

Eq. (2) and (3) are transformed to

$$\frac{\partial \xi}{\partial t} = -\lambda_x \xi + \lambda_i \eta + \gamma_x \sigma_x \varphi - \sigma_x (X^0 \varphi + \phi^0 \xi + \varphi \cdot \xi)\tag{8}$$

$$\frac{\partial \eta}{\partial t} = -\lambda_i \eta + \gamma_i \sigma_x \varphi\tag{9}$$

The buckling term B^2 can be expanded into two parts, one equilibrium part B^{2*} and one perturbation part,

$$B^2(z,t) = B^{2*}(z) + \alpha(z) \varphi(z,t) + \beta \cdot \xi(z,t) + c(z,t) + u(z,t)\tag{10}$$

α and β are coefficients, that express the dependence of B^2 on changes in flux (and temperature) and xenon respectively. c is the influence on buckling from control rod movement and u is a general control term, which is available for the operator.

Assuming the diffusion constant to be space independent ($E = 1$), the one-dimensional diffusion equation can be evaluated in the form

$$\frac{\partial^2 \varphi}{\partial z^2} + (\alpha \varphi + \beta \xi + c + u)(\phi^0 + \varphi) + B^{2*} \cdot \varphi = 0\tag{11}$$

2.2.5 FINITE DIFFERENCES

Finite differences are used to solve the space dependent equations. The laplace operator is approximated by

$$\frac{d^2\varphi}{dz^2} \approx \frac{\varphi_{k+1} - 2\varphi_k + \varphi_{k-1}}{h^2}$$

The neutron equation (11) thus reads:

$$\begin{aligned} \varphi_{k-1} - 2\varphi_k + \varphi_{k+1} + h^2(\alpha_k \varphi_k + \beta \xi_k + c_k + u_k)(\phi_k^0 + \varphi_k) + \\ + h^2 \cdot B_k^{2*} \cdot \varphi_k = 0 \quad k = 1, \dots, N \end{aligned} \quad (12)$$

where k are space points.

The boundary conditions are

$$\varphi_0(t) = \varphi_{N+1}(t) = 0$$

$$\varphi_k(0) = 0 \quad k = 1, \dots, N \quad (13)$$

$$\xi_0(t) = \xi_{N+1}(t) = \eta_0(t) = \eta_{N+1}(t) = 0$$

$$\xi_k(0) = \eta_k(0) = 0 \quad k = 1, \dots, N$$

The power condition is

$$\sum_{j=1}^N K_j \cdot \varphi_j = 0 \quad (14)$$

where all $K_j = 1$ in the simplest case. The xenon and iodine equations for space point k are got from (8) and (9) where we directly can put the subscript k on the variables and ordinary instead of partial derivatives.

2.3 BEHAVIOUR OF THE SOLUTION

Consider a thermal reactor operating at constant power. The introduction of a small tilt in the flux shape, for example from top to bottom, causes the flux to increase at top and decrease at bottom. The burn-out of xenon increases at once in the top (last term in (2)), while the local rates of formation of xenon from iodine decay remain nearly constant for a while (second term in (2)). The xenon burn-out makes the reactivity higher in the top and lower in the bottom. Thus the tilt increases. The peak of the power in the top is limited by the condition of constant total power and by the amount of reactivity, which can be added by the burn-out of xenon.

The growth of neutron flux in the top causes the prompt generation of xenon and iodine directly out of the fissions to increase (third term in (2), last term in (3)). The successive growth of xenon of the radioactive decay of iodine prevents the neutron flux to increase, and the oscillations continue.

Xenon oscillations can occur only at high flux levels, at which the rate of xenon burn-out is important relative to the rate of xenon decay. Likewise, oscillations can occur only in big cores, where the average value of buckling is small. Physically this means that the dimension of the core is much bigger than the migration area. Two or more regions can begin to function as independent nuclear units, i.e. hardly any of the fissions in one region are caused by neutrons born in the other region (see Henry - Germann [5]).

Figure 1 shows the axial flux distribution of a pressurized heavy-water core.

The equilibrium flux has been disturbed by a transport of 0.5% reactivity from bottom to top, while total power is constant.

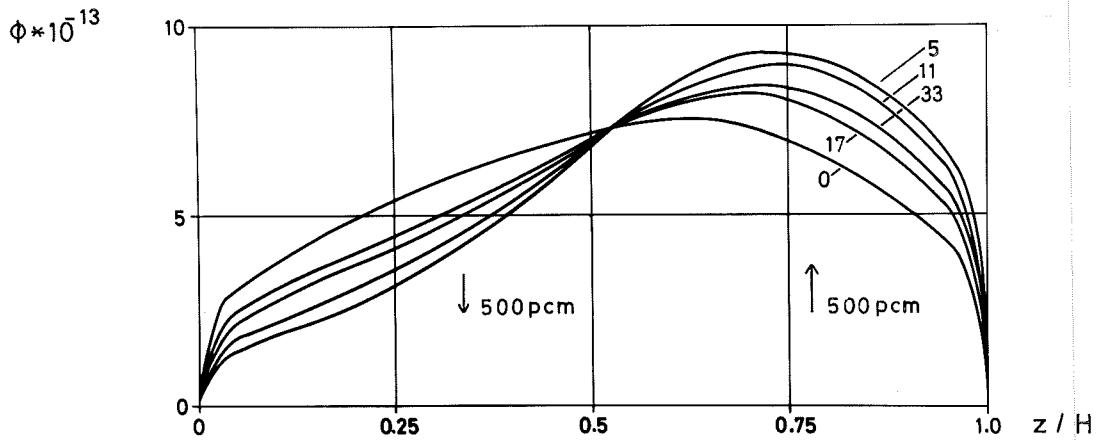


Figure 1. The distribution of neutron flux along the core axis as function of time due to xenon oscillation, calculated with the TRAXEN model. The transient has resulted from a stepwise movement of 0.5% reactivity from one core half to the other.

Core height = 7.0 m

Migration area = 440 cm^2

Mean flux = $5.65 \times 10^{13} \text{ n/cm}^2 \times \text{sec}$

Time in hours is parameter.

2.4 DIFFERENT MATHEMATICAL MODELS USED BY OTHER AUTHORS

2.4.1 LINEAR MODAL EXPANSION MODELS

A number of methods have been used to solve the linearized xenon problem. Among different modal expansion models, two methods are most common, the first one originated by Kaplan [7] - [10], 1961, the other one by Randall - St. John [17], 1958.

The Kaplan modal expansion is the only complete eigenfunction expansion of the state equations and has the form:

$$\omega_m \cdot \mathcal{A}(\tilde{r}) \Psi_m(\tilde{r}) = \mathcal{L}(\tilde{r}) \Psi_m(\tilde{r}) \quad (15)$$

where $\mathcal{A}(\tilde{r})$ and $\mathcal{L}(\tilde{r})$ are spatial operators, which can be real and Hermitian. The state vector is expanded into the modes Ψ_m ,

$$x(\tilde{r}, t) = \sum_0^{\infty} a_m(t) \Psi_m(\tilde{r})$$

and the stability can be calculated.

The Kaplan modes are the "natural" modes to work with, as they are independent of each other, why the mathematical treatment is quite nice. The numerical calculations may, however, be rather involved, and therefore other modes have been used, the clean reactor modes, even called flux shape modes [17].

The variables ϕ , X , I , are expanded in functions $v_i(\tilde{r})$ which are defined by (compare (1) and (10))

$$(\nabla^2 + B^2) v_i + \mu_i^2 v_i = 0 \quad i = 0, 1, \dots \quad (16)$$

where μ_i are the eigenvalues.

Here μ_0 is zero and v_0 is proportional to the unpoisoned (clean) neutron flux. The equation consists solely by Hermitian operators, why the modes can form an orthonormal basis

$$\int_V v_i(\tilde{r}) v_k(\tilde{r}) d^3r = \delta_{ik}$$

The equations for the modal time coefficients here contain infinite sums of cross terms like:

$$\sum_0^{\infty} \int_V \phi^0(\mathbf{r}) v_i(\mathbf{r}) v_k(\mathbf{r}) d^3\mathbf{r}$$

which causes a modal interaction which is high, unless the flux is flat. If the sums are convergent, they can be truncated after a finite number of terms, but this may cause big numerical problems.

However, the clean reactor modes have some attractive features. Their completeness is not in doubt. The modes are rather easy to calculate. They are independent of power level, and have not to be recalculated at each operating point. The specific behaviour of the clean reactor modes are better known than that of the natural modes. Computational results seem to indicate, that the natural mode spectral theory is close to the flux shape mode theory for many real nuclear reactors.

2.4.2 NONLINEAR SPACE INDEPENDENT MODELS

As the xenon equations are non-linear, the linear approximation does not accurately describe bigger deviations from equilibrium. Chernick [1] shows the importance of nonlinear terms in a space independent reactor. Nonlinear stability analysis of a point reactor has also been studied by Smets [20], Gyftopoulos [3] and Sha [18] using Lyapunov's second method.

The neutron equation has the form:

$$\frac{d\phi}{dt} = (a_1 - a_2 X)\phi$$

The existence of periodic solutions can be shown. The nonlinear terms affect the amplitude of the oscillations.

In [15], chapter 5, Olsson shows that a space independent model will give bad results for big disturbances.

2.4.3 DIGITAL AND ANALOG SIMULATIONS

Nonlinear simulations of the xenon oscillations have been performed with analog and digital methods. A survey of references is made, as mentioned previously, by Wiberg [24]. Recent works have been done at Westinghouse [14] with particular emphasis on azimuthal instabilities.

The axial stability problem has been studied by Norinder [13] with clean reactor mode approach and by Stacey [21] with difference approximation approach.

In another report [15] is described results from digital simulations of an axial pressurized water reactor, approximated by finite differences, the TRAXEN model.

2.5 A NONLINEAR SPATIAL DIFFERENCE AXIAL MODEL, THE TRAXEN MODEL

The TRAXEN model is a nonlinear finite difference model, based on one group diffusion theory. The simplifications from 2.1 are even assumed here.

The model is constituted by eq. (1) - (6) or in incremental form by (8), (9), (12), (14). The spatial operator in (1) is approximated by finite differences. The expression for the control rod is uniquely determined by one parameter, the insertion length $\lambda \cdot H$, where $0 \leq \lambda \leq 1$ normally. Then

$$c(z,t) = \lambda \cdot c^1 \quad \lambda < 0, \lambda > 1$$

$$c(z,t) = \begin{cases} c^1 & 0 \leq z \leq \lambda H \\ 0 & \lambda H < z \leq H \end{cases} \quad 0 \leq \lambda \leq 1 \quad (17)$$

where c^1 is constant.

The values $\lambda < 0$, and $\lambda > 1$ are introduced of computational reasons. A negative λ means that reactivity must be added. A big λ means that absorption in the rod must be bigger in order to maintain criticality.

The absorption $c(z,t)$ can also be varied, while the insertion is constant, say z^* , where $0 < z^* < H$. The parameter λ now determines the rate of absorption, and we define

$$c(z,t) = \begin{cases} \lambda \cdot c_1 & z \leq z^* \\ 0 & z > z^* \end{cases} \quad (18)$$

where c_1 is a constant.

If $z^* = H$ we call the control homogeneous.

Physically we can interpret this control as consisting of many fine rods. Only one fine rod is moved at every instant.

In order to study transients, the flux can be disturbed arbitrarily by the term $u(z,t)$, which can be specified in every space point z_i as a polygon chain in time.

A Fortran program TRAXEN is written for this model. The numerical methods and simulation results are reported in [15]. The program is tested for maximum 40 axial meshpoints. The program has been used to compare the results of the analysis of the more simple models, presented in chapter 4 and 5.

2.6 A TWO SPACE POINT AXIAL NONLINEAR MODEL

In order to get a simple description of the xenon problem we approximate the stationary diffusion equation by only two finite space points. The neutron equations then are nothing else than two algebraic conditions. These are combined with the four xenon and iodine equations.

2.6.1 SYSTEM EQUATIONS

The axis of the core is divided into three equal parts. As the boundary conditions (13) must be satisfied the variables are defined in two space points.

We use (12) to write the diffusion equation, and neglect the term $u(z,t)$.

$$\begin{aligned}
 & -2\varphi_1 + \varphi_2 + h^2 \{ (B_1^{2*} + \alpha_1 \phi_1^0) \varphi_1 + c_1 \phi_1^0 + \beta \phi_1^0 \xi_1 + \\
 & + c_1 \varphi_1 + \beta \xi_1 \varphi_1 + \alpha_1 \varphi_1^2 \} = 0
 \end{aligned} \tag{19}$$

$$\begin{aligned}
 & \varphi_1 - 2\varphi_2 + h^2 \{ (B_2^{2*} + \alpha_2 \phi_2^0) \varphi_2 + c_2 \phi_2^0 + \beta \phi_2^0 \xi_2 + \\
 & + c_2 \varphi_2 + \beta \xi_2 \varphi_2 + \alpha_2 \varphi_2^2 \} = 0
 \end{aligned} \tag{20}$$

where the subscripts are space points and the superscript zero stands for equilibrium values.

The constant power condition (14) simply reads:

$$\varphi_1 + \varphi_2 = 0 \tag{21}$$

Let us call

$$g_1 = \frac{3}{h^2} - (B_1^{2*} + \alpha_1 \phi_1^0) \tag{22}$$

$$g_2 = \frac{3}{h^2} - (B_2^{2*} + \alpha_2 \phi_2^0) \tag{23}$$

Equations (21) - (23) are inserted in the algebraic conditions for the flux (19) and (20) which gives:

$$\alpha_1 \varphi_1^2 + \varphi_1 [\beta \xi_1 + c_1 - g_1] + \phi_1^0 (c_1 + \beta \xi_1) = 0 \tag{24}$$

$$\alpha_2 \varphi_1^2 + \varphi_1 [-\beta \xi_2 - c_2 + g_2] + \phi_2^0 (c_2 + \beta \xi_2) = 0 \tag{25}$$

In addition we have an algebraic condition on the control c_k (compare (17) and (18)):

$$f(c_1, c_2) = 0 \quad (26)$$

The xenon and iodine equations, (8), (9), with (21) inserted, are written

$$\frac{d\xi_1}{dt} = (-\lambda_x - \sigma_x \phi_1^0) \xi_1 + \lambda_i \eta_1 + \sigma_x (\gamma_x - X_1^0) \varphi_1 - \sigma_x \varphi_1 \xi_1 \quad (27)$$

$$\frac{d\xi_2}{dt} = (-\lambda_x - \sigma_x \phi_2^0) \xi_2 + \lambda_i \eta_2 - \sigma_x (\gamma_x - X_2^0) \varphi_1 + \sigma_x \varphi_1 \xi_2 \quad (28)$$

$$\frac{d\eta_1}{dt} = -\lambda_i \eta_1 + \gamma_i \sigma_x \varphi_1 \quad (29)$$

$$\frac{d\eta_2}{dt} = -\lambda_i \eta_2 - \gamma_i \sigma_x \varphi_1 \quad (30)$$

Out of (24) - (26) we can solve φ_1 as a function of ξ_1 and ξ_2 . Eq. (27) - (30) therefore constitutes a fourth order nonlinear dynamic system.

As state variables we choose:

$$\boxed{x_1 = \xi_1 \quad x_2 = \eta_1 \quad x_3 = \xi_1 + \xi_2 \quad x_4 = \eta_1 + \eta_2} \quad (31)$$

and the system equations read:

$$\frac{dx_1}{dt} = (-\lambda_x - \sigma_x \phi_1^0) x_1 + \lambda_i x_2 + \sigma_x (\gamma_x - X_1^0) \varphi_1 - \sigma_x \varphi_1 x_1 \quad (32)$$

$$\frac{dx_2}{dt} = -\lambda_i x_2 + \gamma_i \sigma_x \varphi_1 \quad (33)$$

$$\begin{aligned} \frac{dx_3}{dt} = & \sigma_x (\phi_2^0 - \phi_1^0) x_1 + (-\lambda_x - \sigma_x \phi_2^0) x_3 + \lambda_i x_4 + \\ & + \sigma_x (X_2^0 - X_1^0) \varphi_1 + \sigma_x \varphi_1 [x_3 - 2x_1] \end{aligned} \quad (34)$$

$$\frac{dx_4}{dt} = -\lambda_i x_4 \quad (35)$$

where $\varphi_1 = \varphi_1(x_1, x_3)$.

The system is thus constituted by the equations (32) - (35) and (24) - (26).

If the equilibrium neutron flux is assumed to be symmetric and the buckling coefficient α space independent we get from (22) and (23)

$$\begin{aligned} g_1 &= g_2 = g \\ X_1^0 &= X_2^0 = X^0 \\ \phi_1^0 &= \phi_2^0 = \phi^0 \end{aligned} \quad (36)$$

The system equations (32) - (35) are then simplified to

$$\frac{dx_1}{dt} = (-\lambda_x - \sigma_x \phi^0) x_1 + \lambda_i x_2 + \sigma_x (\gamma_x - X^0) \varphi_1 - \sigma_x \varphi_1 x_1 \quad (37)$$

$$\frac{dx_2}{dt} = -\lambda_i x_2 + \gamma_i \sigma_x \varphi_1 \quad (38)$$

$$\frac{dx_3}{dt} = (-\lambda_x - \sigma_x \phi^0) x_3 + \lambda_i x_4 + \sigma_x \varphi_1 (x_3 - 2x_1) \quad (39)$$

$$\frac{dx_4}{dt} = -\lambda_i x_4 \quad (40)$$

where $\varphi_1 = \varphi_1(x_1, x_3)$ is found from (24) - (26) with (36) inserted.

2.6.2 NEUTRON FLUX EQUATIONS AT DIFFERENT CONTROL TYPES AND SYMMETRIC EQUILIBRIUM FLUX

In order to express the neutron flux in the state variables, we must solve (24) - (26). In this study, we shall regard two cases, called the rod control and the homogeneous control cases.

In order to simulate a rod movement, we assume that the absorption c is varying in one point. This means physically, that the rod is assumed to oscillate only in one half of the core.

When the absorption is equal in the two points we define the control to be homogeneous.

ROD CONTROL

The absorption $c_k(t)$, (12), (24) and (25), is acting only in point one, why (26) is simplified to:

$$c_2 = 0 \tag{41}$$

Eq. (25) gives φ_1 as a function of $\xi_2 = x_3 - x_1$ (see (31)),

$$\varphi_1 = \varphi_1(x_3 - x_1)$$

$$\varphi_1 = \frac{\beta(x_3 - x_1) - g}{2\alpha} \left\{ 1_{(\mp)} \sqrt{1 - \frac{4\alpha \phi^0 \beta(x_3 - x_1)}{[g - \beta(x_3 - x_1)]^2}} \right\} \tag{42}$$

The plus sign is skipped of physical reasons because both x_3 , x_1 and φ_1 shall be zero at equilibrium.

If the temperature coefficient α equals zero we get

$$\varphi_1 = \frac{\phi^0 \beta(x_3 - x_1)}{\beta(x_3 - x_1) - g} \tag{43}$$

When solving the flux equilibrium equation (2) in the symmetric case we find directly:

$$\xi_1 = \xi_2 = g = \frac{2}{h^2} - \alpha \phi^0 \tag{44}$$

HOMOGENEOUS CONTROL

The absorption term c_k is now constant for all k , why (26) reads:

$$c_1 - c_2 = 0 \tag{45}$$

Eq. (24) - (25) then gives a third degree equation in φ_1 to be solved.

$$2\alpha \varphi_1^3 + \varphi_1^2 \beta(2x_1 - x_3) + 2g \phi^0 \varphi_1 - (\phi^0)^2 \beta(2x_1 - x_3) = 0 \tag{46}$$

where g is defined by (44).

With the temperature control $\alpha = 0$ we get the flux equation:

$$\varphi_1^2 + \frac{2g \phi^0}{\beta(2x_1 - x_3)} \varphi_1 - (\phi^0)^2 = 0 \tag{47}$$

These equations define an unique value of φ_1 of the same physical reason as (42).

2.7 A LINEARIZED TWO SPACE POINT MODEL

The two point model gets very attractive when the equations are linearized. We show that the Lyapunov - Poincaré theorem is valid for the model.

After the system equations for the asymmetric equilibrium flux shape are derived, we simplify to the symmetric equilibrium flux. Here stability is independent of control type. We also show that the fourth order system matrix is of a special simple form. Two eigenvalues are constant for all core parameters, and the two other eigenvalues are calculated directly from a second order submatrix.

2.7.1 LINEARIZATION OF SYSTEM EQUATIONS

The model is constituted by the eq. (32) - (35) and (42), (43) or (46), (47).

As the nonlinearities can be represented by higher order terms the system equations can be written:

$$\dot{x} = A x + \Gamma(x)$$

where the vector function $\Gamma(x)$ has the properties

$$\Gamma(0) = 0$$

$$\lim_{\|x\| \rightarrow 0} \frac{\|\Gamma(x)\|}{\|x\|} = 0$$

$$\|x\| = 0$$

Consequently, the Lyapunov - Poincaré theorem can be applied.

In this section we will find expressions for the system matrix A.

2.7.2 THE LINEARIZED NEUTRON FLUX EQUATION AND THE SYSTEM EQUATIONS FOR ASYMMETRIC FLUX

CONTROL ROD ACTION IN ONE SPACE POINT

Skipping products of the incremental variables in (24), (25) and assuming rod control as in (41),

$$c_2 = 0$$

we get from (25)

$$\varphi_1 = \frac{\phi_2^0}{g_2} \beta(x_1 - x_3) \tag{48}$$

Eq. (48) is inserted into (32) - (35) where all products of the state variables are neglected. The system equations then have the form:

$$\frac{dx}{dt} = A_1 x \quad \text{where}$$

$$A_1 = \begin{bmatrix} -\lambda_x - \sigma_x \frac{\phi_1^0}{g_2} - \frac{\sigma_x (X_1^0 - \gamma_x) \phi_2^0 \beta}{g_2} & \lambda_i + \frac{\sigma_x (X_1^0 - \gamma_x) \phi_2^0 \beta}{g_2} & 0 \\ \gamma_i \sigma_x \frac{\phi_2^0 \beta}{g_2} & -\lambda_i - \gamma_i \sigma_x \frac{\phi_2^0 \beta}{g_2} & 0 \\ \sigma_x \left[(\phi_2 - \phi_1) + \frac{(X_2^0 - X_1^0) \phi_2^0 \beta}{g_2} \right] & 0 & -\lambda_x - \sigma_x \frac{\phi_2^0 - \sigma_x}{g_2} - \frac{(X_2^0 - X_1^0) \phi_2^0 \beta}{g_2} \\ 0 & 0 & 0 \end{bmatrix} \quad (49)$$

and x is defined in (31).

HOMOGENEOUS CONTROL

Here we state

$$c_1 = c_2 = c \quad (\text{see (26) and (45)})$$

By adding (24) and (25) and neglecting products of the increments ξ_i, φ_i, c we get:

$$\varphi_1 = \frac{\beta(2x_1 - x_3)}{\mathcal{H}} \quad (50)$$

where we have defined:

$$\mathcal{H} = \frac{g_1}{\phi_1^0} + \frac{g_2}{\phi_2^0} \quad (51)$$

The system equations (32) - (35) are now simplified to:

$$\frac{dx}{dt} = A_2 x$$

where

$$A_2 = \begin{bmatrix} -\lambda_x - \sigma_x \phi_1^0 - \frac{2\sigma_x (X_1^0 - \gamma_x)\beta}{\mathcal{L}} & \lambda_i & \frac{\sigma_x (X_1^0 - \gamma_x)\beta}{\mathcal{L}} & 0 \\ \gamma_i \sigma_x \frac{2\beta}{\mathcal{L}} & -\lambda_i & -\gamma_i \sigma_x \frac{\beta}{\mathcal{L}} & 0 \\ \sigma_x \left[(\phi_2^0 - \phi_1^0) + \frac{2(X_2^0 - X_1^0)\beta}{\mathcal{L}} \right] & 0 & -\lambda_x - \sigma_x \phi_2^0 - \frac{\sigma_x (X_2^0 - X_1^0)\beta}{\mathcal{L}} & \lambda_i \\ 0 & 0 & 0 & -\lambda_i \end{bmatrix} \quad (52)$$

2.7.3 THE LINEARIZED SYSTEM EQUATIONS FOR SYMMETRIC FLUX

If the equilibrium flux is symmetric, the system equations are rather attractive.

CONTROL ROD IN ONE SPACE POINT

If the control rod is affecting space point one, the system matrix A_1 (49) is simplified to:

$$A_3 = \begin{bmatrix} -\lambda_x - \sigma_x \phi^0 - \frac{\sigma_x (X^0 - \gamma_x)\phi^0 \beta}{g} & \lambda_i & \frac{\sigma_x (X^0 - \gamma_x)\phi^0 \beta}{g} & 0 \\ \gamma_i \sigma_x \frac{\phi^0 \beta}{g} & -\lambda_i & -\gamma_i \sigma_x \frac{\phi^0 \beta}{g} & 0 \\ 0 & 0 & -\lambda_x - \sigma_x \phi^0 & \lambda_i \\ 0 & 0 & 0 & -\lambda_i \end{bmatrix} \quad (53)$$

where (36) is taken into account.

HOMOGENEOUS CONTROL

Homogeneous control leads to the system matrix out of A_2 (52) and the matrix looks like:

$$A_4 = \begin{bmatrix} -\lambda_x - \sigma_x \phi^0 - \frac{\sigma_x (X^0 - \gamma_x) \beta \phi^0}{g} & \lambda_i & \frac{\sigma_x (X^0 - \gamma_x) \beta \phi^0}{2g} & 0 \\ \gamma_i \sigma_x \frac{\phi^0 \beta}{g} & -\lambda_i & -\gamma_i \sigma_x \frac{\beta \cdot \phi^0}{2g} & 0 \\ 0 & 0 & -\lambda_x - \sigma_x \phi^0 & \lambda_i \\ 0 & 0 & 0 & -\lambda_i \end{bmatrix} \quad (54)$$

The only difference between A_3 and A_4 occurs in the elements a_{13} and a_{23} .

The characteristic equations are:

$$\begin{aligned} |sI - A_3| &= (s - a_{44})(s - a_{33}) [(s - a_{11})(s - a_{22}) - a_{12} \cdot a_{21}] = \\ &= |sI - A_4| \end{aligned}$$

As the two eigenvalues:

$$\begin{aligned} s_1 &= a_{44} = -\lambda_i \\ s_2 &= a_{33} = -\lambda_x - \sigma_x \phi^0 \end{aligned} \quad (55)$$

are always negative and real, we need only study the 2x2 matrix

$$\begin{bmatrix} a_{11} & a_{12} \\ a_{21} & a_{22} \end{bmatrix}$$

in the stability analysis.

This 2x2 matrix can be derived in another way, which can give a physical interpretation. If the absorption terms c_1 are neglected in the flux equations (24), (25), we get only three state variables x_1, x_2, x_4 , as x_3 is uniquely determined by x_1 . The system equations are now

$$\frac{d}{dt} \begin{pmatrix} x_1 \\ x_2 \\ x_4 \end{pmatrix} = \begin{pmatrix} a_{11} & a_{12} & 0 \\ a_{21} & a_{22} & 0 \\ 0 & 0 & -\lambda_i \end{pmatrix} \begin{pmatrix} x_1 \\ x_2 \\ x_4 \end{pmatrix} \quad (56)$$

where the elements of the matrix are the same as the corresponding terms in A_3 (53) and A_4 (54).

Thus, it is permitted in stability analysis to neglect the rod influence in the symmetric, linear model.

2.8 A LINEAR SPACE DIFFERENCE MULTIPOINT MODEL

In this section is derived a linearized version of the TRAXEN finite difference model. We can simply show that the rod insertion is uniquely determined, why one rod is not sufficient to control the oscillations. In the special case a flat equilibrium flux we prove that stability is independent of control type.

2.8.1 GENERAL SYSTEM EQUATIONS

The linearized xenon and iodine equations are simply got from (8) and (9):

$$\frac{d\xi_k}{dt} = -\lambda_x \xi_k + \lambda_i \eta_k + \gamma_x \sigma_x \varphi_k - \sigma_x (X_k^0 \varphi_k + \Phi_k^0 \xi_k) \quad (57)$$

$$\frac{d\eta_k}{dt} = -\lambda_i \eta_k + \gamma_i \sigma_x \varphi_k \quad k = 1, \dots, N \quad (58)$$

where the subscripts stand for space point.

The linearized diffusion equation for the neutron flux in space point k is derived directly from (12) with $u(z,t) = 0$,

$$\varphi_{k-1} + \varphi_{k+1} + \varphi_k [-2 + h^2 (B_k^{2*} + \alpha \phi_k^0)] + h^2 \phi_k^0 [c_k + \beta \xi_k] = 0$$

$$k = 1, \dots, N \quad (59)$$

with the boundary conditions (13) and the power condition (14), which we simplify to:

$$\sum_{i=1}^N \varphi_i = 0 \quad (60)$$

As pointed out in (17), the control terms c_k are determined by one parameter, the insertion length of the rod, or by the homogeneous absorption (18). This means, that the unknown parameters c_1, \dots, c_N are connected by $N-1$ conditions.

$$f_i(c_1, \dots, c_N) = 0 \quad i = 1, \dots, N-1 \quad (61)$$

Now, to express the N variables φ_k in the state variables ξ_k and η_k we have $2N$ equations (59) - (61) for the $2N$ unknown parameters c_k and φ_k . This simple calculus shows directly that the rod insertion is uniquely determined in every moment, if the total power is to be held constant. Thus the system is not controllable by one rod.

2.8.2 SPECIAL CASE I: FLAT EQUILIBRIUM FLUX

In this section we will prove, that the stability of the flat flux is independent of the control term c . Thus, we can simply neglect the absorption c , when analyzing the stability of the flat flux.

In order to get a suitable representation of the system, let us add all the ξ_k -equations (57) and the η_k -equations (58). As all X_k^0 and ϕ_k^0 are constant for all k and because of (60) we get at once:

$$\frac{d}{dt} \left(\sum_1^N \xi_k \right) = (-\lambda_x - \sigma_x \phi^0) \left(\sum_1^N \xi_k \right) + \lambda_i \sum_1^N \eta_k \quad (62)$$

$$\frac{d}{dt} \left(\sum_1^N \eta_k \right) = -\lambda_i \left(\sum_1^N \eta_k \right) \quad (63)$$

Let us now define the state vector x with the components:

$$\begin{aligned} x_1 &= \xi_1 & x_2 &= \eta_1 & x_{2i-1} &= \xi_i & x_{2i} &= \eta_i \\ x_{2N-1} &= \sum_1^N \xi_i & x_{2N} &= \sum_1^N \eta_i \end{aligned}$$

The system dynamics can now be represented by

$$\frac{dx}{dt} = A_N \cdot x$$

where the $2N \times 2N$ matrix A_N can be partitioned into:

$$A_N = \begin{bmatrix} A_{N-1} & | & B \\ \hline 0 & | & \begin{matrix} a_1 & a_2 \\ 0 & a_3 \end{matrix} \end{bmatrix} \quad (64)$$

where A_{N-1} is a $[2(N-1)] \times [2(N-1)]$ matrix, B is a $2(N-1) \times 2$ matrix as we can see from (62) and (63).

The eigenvalues of A_N are the same as those of A_{N-1} plus the eigenvalues a_1 and a_3 which are always negative and real, (62) - (63)

$$a_1 = -\lambda_x - \sigma_x \phi^0$$

$$a_3 = -\lambda_i$$

For the flat flux we get a simple form of the flux equation. As the diffusion equation (1) must be satisfied at equilibrium, where

$$\bar{\phi} = \frac{1}{N} \sum_{k=1}^N \phi_k = \frac{1}{N} \cdot N \cdot \phi_k^0 = \phi_k^0 \quad k = 1, \dots, N \quad (65)$$

we get directly the conditions

$$h^2 B_k^{2*} = \begin{cases} 0 & 2 \leq k \leq N-1 \\ 1 & k = 1, k = N \end{cases} \quad (66)$$

We use (66) and (65) for all k, and (59) is simplified to:

$$\varphi_{k-1} + \varphi_{k+1} + \varphi_k (-2 + h^2 \alpha \phi^0) + h^2 \phi^0 (c_k + \beta \xi_k) = 0 \quad (67)$$

$$2 \leq k \leq N-1$$

For k = 1 and k = N we get respectively:

$$\varphi_2 + \varphi_1 [-1 + h^2 \alpha \phi^0] + h^2 \phi^0 (c_1 + \beta \xi_1) = 0 \quad (68)$$

$$\varphi_{N-1} + \varphi_N [-1 + h^2 \alpha \phi^0] + h^2 \phi^0 (c_N + \beta \xi_N) = 0 \quad (69)$$

Now, let us add the flux equations (67) - (69) for k = 1, 2, ..., N.

We get, using (60):

$$\sum_1^N c_k + \beta \sum_1^N \xi_k = 0 \quad (70)$$

This equation will be used in following section.

CONTROL ROD ACTION

With a control rod inserted to space point number k we can simplify the control to the expression:

$$\begin{aligned} c_1 &= c_2 = \dots = c_{k-1} = 0 \\ c_k &= c \\ c_{k+1} &= \dots = c_N = 0 \end{aligned} \quad (71)$$

Physically, this means that the rod is inserted in equilibrium from point zero to space point k-1. The rod absorption is included in the undisturbed buckling term B_k^{2*} . We assume that the rod moves just around point k, where the absorption is varied with c.

Eq. (70) gives directly:

$$c = -\beta \sum_1^N \xi_k = -\beta \cdot x_{2N-1} \quad (72)$$

Eq. (72) is inserted in (67) - (69) which reads:

$$\begin{bmatrix} q_1 & -1 & 0 \dots & 0 \\ -1 & q & -1 & 0 \dots \\ 0 & -1 & q & -1 & 0 \\ & & & & \cdot \\ & & & & \cdot \\ & & & & \cdot \\ & & & & \cdot \\ & & & & \cdot \\ & & & & \cdot \\ & & & & \cdot \\ & & & & \cdot \\ & & & q & -1 \\ 0 \dots & 0 & -1 & q_1 \end{bmatrix} \varphi = h^2 \phi^0 \beta \begin{bmatrix} \xi_1 \\ \cdot \\ \cdot \\ \cdot \\ \cdot \\ \xi_{k-1} \\ \xi_k - \sum_1^N \xi_u \\ \xi_{k+1} \\ \cdot \\ \cdot \\ \cdot \\ \xi_N \end{bmatrix} \quad (73)$$

or in matrix form

$$G \cdot \varphi = h^2 \phi^0 \beta \xi^*$$

where we have defined

$$\begin{aligned} q_1 &= 1 - h^2 \alpha \phi^0 \\ q &= 2 - h^2 \alpha \phi^0 \end{aligned} \quad (74)$$

and ξ^* stands for the altered ξ -vector in (73).

The flux vector can be solved from (73)

$$\varphi = h^2 \cdot \phi^0 \cdot \beta \cdot G^{-1} \cdot \xi^* = R \cdot \xi^*$$

where R is a NxN matrix, or in scalar form

$$\varphi_i = \sum_{j=1}^N r_{ij} \cdot \xi_j - r_{ik} \cdot \left(\sum_{v=1}^N \xi_v \right) \quad i = 1, \dots, N \quad (75)$$

Now, let us neglect the term c from the beginning. This will make the system one state variable less, as (59), (60) now gives $N+1$ conditions for the N unknown φ_k . Thus we exclude

$$x_{2N-1} = \sum_{v=1}^N \xi_v$$

which can be calculated from the other state variables. From (72) we see, that

$$x_{2N-1} = 0$$

In (73) the vector ξ^* changes to ξ , while all the coefficients r_{ij} in (75) are unaltered. The last term in (75) is now lost and the equation reads:

$$\varphi_i = \sum_{j=1}^N r_{ij} \xi_j \quad i = 1, \dots, N \quad (76)$$

Comparing (75) and (76) we see that the partition matrix A_{N-1} in (65) is unaffected if (76) is inserted instead of (75) in (57) and (58). We exclude eq. number $(2N-1)$ and the first column in B , but this does not change the eigenvalues of A_{N-1} and the stability.

HOMOGENEOUS CONTROL

A homogeneous control gives a similar result. Instead of (71) we now assume:

$$c_1 = c_2 = \dots = c_N = c \quad (77)$$

and out of eq. (70) we get:

$$c = -\frac{\beta}{N} \sum_{k=1}^N \xi_k = -\frac{\beta}{N} \cdot x_{2N-1} \quad (78)$$

The right hand side of (73) is altered to

$$h^2 \phi^0 \beta \begin{bmatrix} \xi_1 - \frac{1}{N} \sum_{k=1}^N \xi_k \\ \vdots \\ \xi_N - \frac{1}{N} \sum_{k=1}^N \xi_k \end{bmatrix} \quad (79)$$

and eq. (75) is altered to

$$\varphi_i = \sum_{j=1}^N r_{ij} \xi_j - (\sum_j r_{ij}) \cdot \frac{1}{N} \sum_k \xi_k \quad i = 1, \dots, N \quad (80)$$

Even here the matrix A_{N-1} is only affected by the first term in (80) and the last term has influence only on the B-matrix in (65). This does not influence on the eigenvalues of A_N .

As in the rod case we lose one state variable when we assume $c = 0$. From (78) we conclude that:

$$x_{2N-1} \equiv 0$$

why eq. number $2N-1$ in (65) is excluded. The matrix A_{N-1} is unaltered if c is neglected, because the last term in (80), which is zero for $c = 0$ does not affect A_{N-1} . B is altered to a $(2N-2) \times 1$ matrix and has no influence on the stability of A_N .

Out of these results, we can neglect the rod in this linear flat flux case, when analyzing stability.

Only $2N-1$ state variables describe the system and stability is determined by $2N-2$ eigenvalues.

2.8.3 SPECIAL CASE II
SINUSOIDAL EQUILIBRIUM FLUX

In this section we present an analytical expression of the constant buckling as a function of the number of meshpoints.

In the continuous case we can easily find a sinusoidal flux as the solution of the neutron flux equation

$$\frac{d^2 \phi}{dz^2} + B_0^2(z) \cdot \phi = 0$$

where the buckling $B_0^2 = \frac{\pi^2}{H^2} = \text{constant}$. (81)

When using finite space differences we get an approximation of the sinusoidal flux by assuming the buckling

$$B_k^2 = B_k^{2*} = \text{constant} \quad k = 1, \dots, N$$

The flux equations are in equilibrium

$$\phi_{k-1} - 2\phi_k + \phi_{k+1} + h^2 B_k^{2*} \phi_k = 0 \quad (82)$$

or in matrix form:

$$\begin{bmatrix} p & -1 & 0 & \dots \\ -1 & p & -1 & 0 & \dots \\ 0 & -1 & p & & \\ & & & & \\ 0 & \dots & & 0 & -1 & p \end{bmatrix} \phi = 0 \quad (83)$$

or $R^* \cdot \phi = 0$

where $p = 2 - h^2 B_k^{2*}$ and the matrix R^* is of order $N \times N$.

In order to get a solution we must require:

$$\det R^* = D_n = 0$$

D_n can be found recursively

$$D_n = p D_{n-1} - D_{n-2} \quad (84)$$

Out of this difference equation we can solve the roots p and we find:

$$p^{(k)} = 2 \cos \frac{\pi k}{N+1} \quad k = 1, \dots, N$$

and thus

$$B_k^{2*} = \frac{2}{h^2} \left(1 - \cos \frac{\pi k}{N+1} \right) \quad (85)$$

where $h = \frac{H}{N+1}$

We can see that B_k^{2*} asymptotically converges to (81).

The flux equations are defined from (59) - (61), where eq. (59) can be written in matrix form

$$\begin{bmatrix} q_1^* & -1 & & & \\ -1 & q_2^* & -1 & & 0 \\ & & \ddots & & \\ 0 & & & -1 & \\ & & -1 & & q_N^* \end{bmatrix} \varphi = h^2 \cdot \begin{bmatrix} \phi_1^0(c_1 + \beta \xi_1) \\ \vdots \\ \phi_N^0(c_N + \beta \xi_N) \end{bmatrix} \quad (86)$$

where $q_i^* = 2 - h^2(B_i^{2*} + \alpha \phi_i^0)$ $i = 1, \dots, N$

The equilibrium flux ϕ_i^0 is found from (83) and B_i^{2*} is defined in (85).

We also define the mean flux:

$$\bar{\phi} = \frac{1}{N+1} \sum_{i=1}^N \phi_i^0 = \text{constant} \quad (87)$$

(Compare (65))

3. PHYSICAL AND TECHNOLOGICAL CONSIDERATIONS

3.1 CRITERION OF STABILITY - PRACTICAL STABILITY

When studying the xenon oscillations, we are concerned with deviations, $\delta\chi$, about some equilibrium state χ^0 , where χ represents a spatially dependent state vector containing iodine, xenon and flux as components.

Stability is used here in the sense of asymptotic stability. This is defined as an asymptotic return to the equilibrium state after initial perturbations, that is

$$\lim_{t \rightarrow \infty} |\delta\chi| = 0$$

Otherwise the trajectory is unstable.

All the linear difference models have well-defined stability criteria. They can be written in the matrix form

$$\frac{dx}{dt} = Ax$$

where the biggest eigenvalue determines the stability. As the geometrical dimensions are strongly connected to stability, it is common in the one-dimensional case to define the critical core height. This one is reached when the biggest eigenvalue has a zero real part. Thus, the degree of stability for a certain set of core parameters can be described either by the eigenvalues or by critical height.

In the nonlinear description we must care about the single trajectories. The nonlinear terms fulfill the conditions for the Lyapunov - Poincaré theorem, so we know that if the linear approximation is asymptotic stable, even the nonlinear zero solution is stable.

A practical stability criterion except the asymptotic stability criterion, which is often used, is the maximum amplitude of an oscillation following a certain serious disturbance. Even if a trajectory is stable it might be forbidden of technological reasons. The flux in one point must not deviate more than a certain amount from the nominal level, and this boundary depends on thermal margins, burn out risk, boiling of the moderator and burn up of the fuel.

3.2 CHOICE OF REACTOR CORE PARAMETERS

The numerical values of all the nuclear and core parameters are found in appendix 1. The core parameters are taken from the Marviken heavy water reactor, whose most significant data are:

core height, including extrapolated boundaries	H = 5.02 m
form factor, axial	$\Psi = 1.35$
temperature coefficient	$\alpha = - 0.226\%$
reactively bounded in fuel, when neutron flux is doubled	
mean flux level	$\bar{\phi} = 5.65 \cdot 10^{13}$ neutr./cm ² ·sec.

The most interesting core parameters to study are

- core height H
- temperature coefficient α
- flux form Ψ
- mean flux level $\bar{\phi}$
- reactivity disturbance distributions

When a parameter is not specially mentioned it has the standard value.

In order to compare the results from two point model analysis with other models, two flux forms are used, namely flat flux ($\Psi = 1.0$) and sinusoidal flux ($\Psi = \frac{\pi}{2}$).

More realistic flux forms have been used in the TRAXEN model in order to study practical situations [15].

3.3 TYPICAL DISTURBANCES

As the reactor dynamics is nonlinear the type of disturbance is very important, when examining the stability. Both amplitude and direction determines the convergence.

As the xenon instability problem mainly is reflected in the first overtone of the flux, it is intuitively clear, that a disturbance of the first overtone is a severe disturbance, which means that reactivity is transferred from the upper core to the lower core or vice versa. An oscillation, thus, can be induced by a slight movement of a control rod or by a refuelling process. A fuel element or a control rod which accidentally falls into the core can induce big disturbances. Thus, a 500 pcm (0.5%) reactivity movement from one half to the other seems to be realistic.

The sensitivity of the flux to different disturbances is discussed in more detail in [15].

4. LINEAR STABILITY ANALYSIS

The linear stability analysis is carried out of two different models, the two point model and the multipoint model, which both are based on finite differences.

In chapter 4.1 is made a simple analysis of the eigenvalues of the two point model as functions of different core parameters. Two eigenvalues are independent of core parameters, and the other two can simply be solved out of a second order submatrix.

The locus of the two most significant eigenvalues for variable core height shows, that the eigenvalues near the stability limit are complex conjugate. It is also shown that critical height of the core has a minimum when mean flux is increased. This is also verified by more complex models.

The critical height is shown to be bigger if the equilibrium flux deviates from a symmetric shape.

In section 4.2 is calculated the critical core height when the number of space points for the neutron equation is increased. The critical height converges to different values, depending on flux shape. The two most significant eigenvalues are all the time complex conjugate near the critical height.

In 4.3 is compared the results from different models. The behaviour of the two point model is verified qualitatively by other models, which are more complex. The results of the multipoint models are compared to the TRAXEN model and a modal expansion model.

4.1 THE TWO POINT FLUX MODEL STABILITY

4.1.1 INFLUENCE OF CORE PARAMETERS

In section 2.7.3 we found that it is only necessary to examine the eigenvalues of the matrix ((2:53), (2:54))

$$A = \begin{pmatrix} -\lambda_x - \sigma_x \phi^0 - \frac{\sigma_x (X^0 - \gamma_x) \phi^0 \beta}{g} & \lambda_i \\ \gamma_i \sigma_x \frac{\phi^0 \beta}{g} & -\lambda_i \end{pmatrix} = \begin{pmatrix} a_{11} & a_{12} \\ a_{21} & a_{22} \end{pmatrix} \quad (1)$$

in order to analyse stability of the symmetric flux.

The eigenvalues are simply calculated to:

$$s = \frac{a_{11} + a_{22}}{2} \pm \sqrt{\frac{(a_{11} + a_{22})^2}{4} - a_{11} a_{22} + a_{12} a_{21}} \quad (2)$$

The two conditions for stability are:

i) $a_{11} + a_{22} < 0$ or

$$\lambda_x + \sigma_x \phi^0 + \frac{\sigma_x}{g} (X^0 - \gamma_x) \phi^0 \beta + \lambda_i > 0 \quad (3)$$

ii) $a_{11} a_{22} - a_{12} a_{21} > 0$ or

$$\lambda_i \left\{ -\lambda_x - \sigma_x \phi^0 - \frac{\sigma_x}{g} (X^0 - \gamma_x) \phi^0 \beta + \gamma_i \sigma_x \frac{\phi^0 \beta}{g} \right\} < 0 \quad (4)$$

As $\gamma_i + \gamma_x = 1$ by definition eq. (4) can be simplified to:

$$\lambda_x + \sigma_x \phi^0 - \frac{\sigma_x}{g} \phi^0 \beta (1 - X^0) > 0 \quad (5)$$

As $\beta < 0$ and $X^0 \leq 1$ this condition is always fulfilled. The stability is thus determined only by (3). It is simply realized from (4), that the eigenvalues are always situated at the same side of the imaginary axis.

(i) CORE HEIGHT INFLUENCE

The eigenvalues (2) are plotted as function of the core height in meter in fig. 1, where we have used the numerical values from section 3.2 and appendix 1. We find the critical core height to be $H = 6.93$ m. Asymptotically the eigenvalues converge to:

$$s = \begin{cases} -\lambda_x - \sigma_x = -0.545 \\ -\lambda_i = -0.106 \end{cases}$$

as H tends to zero.

When H increases to infinity the limits depend primarily on the temperature coefficient α

when $\alpha = 0$ the limits are 0 and ∞

when $\alpha < 0$ the limits are $a > 0$ and $b < \infty$ (see fig. 1)

The condition for oscillations to occur is formulated from (2).

$$a_{11} a_{22} - a_{12} a_{21} - \frac{(a_{11} + a_{22})^2}{4} > 0 \quad \text{or}$$

$$\left[-\lambda_x + \lambda_i - \sigma_x \phi^0 + \frac{\sigma_x (\gamma_x - X^0) \phi^0 \beta}{g} \right]^2 + 4\lambda_i \frac{\sigma_x \gamma_i \phi^0 \beta}{g} < 0$$

For $\phi^0 = 1$, $\alpha = -0.0514$ we get the condition for oscillations:

$$3.24 \leq H \leq 10.1 \quad (\text{m})$$

(see fig. 1)

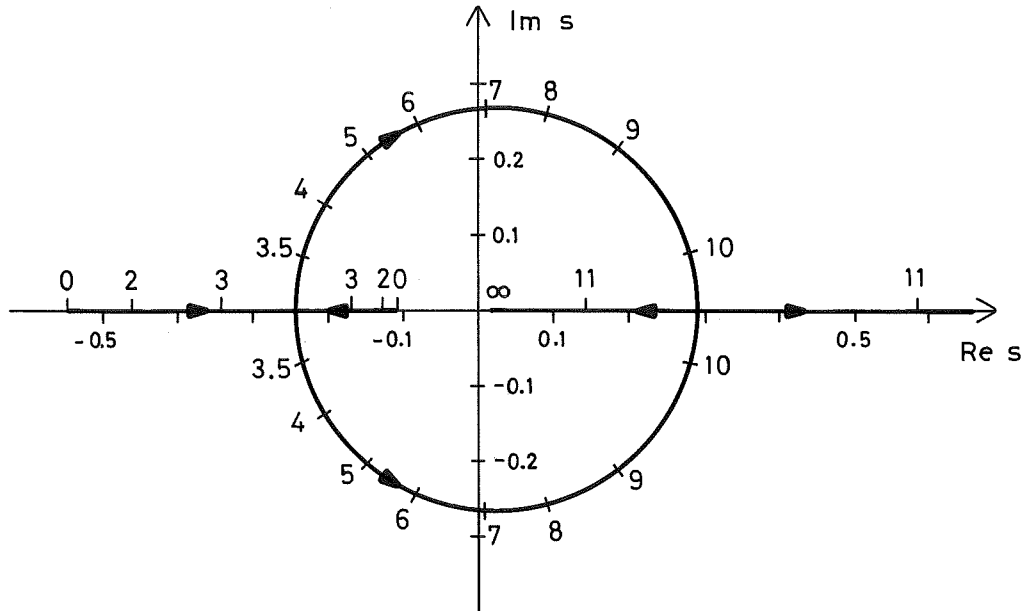


Figure 1. The locus of the two most significant eigenvalues of the linearized symmetric two point model. (2:53-54).
 The parameter is core height (m).
 Mean flux $\bar{\phi} = 1.0$
 Temp. coeff. $\alpha = -0.0514$

(ii) PERIOD TIME

The period for the oscillations at the stability limit is found from (2):

$$T = \frac{2\pi}{\sqrt{a_{11} a_{22} - a_{12} a_{21}}} = \frac{2\pi}{\left[\lambda_x \left(\lambda_x + \sigma_x \phi^0 + \frac{\sigma_x (X^0 - 1) \phi^0 \beta}{g} \right) \right]^{1/2}} \quad (6)$$

The argument of the root is always positive, which means that if the reactor is at the stability limit the eigenvalues are always complex conjugate. The period is found to be

$$T = 23.8 \text{ h.}$$

at the stability limit, where

$$H = 6.93 \text{ m}$$

From (6) it is easily verified that T decreases when ϕ^0 increases. The last term in the denominator in (6) is slow varying with ϕ^0 . The coefficients

$$\frac{(X^0 - 1)\beta}{g} \sim 0.05 \text{ why we have } \frac{\sigma_X(X^0 - 1)\beta \phi^0}{g} \sim 0.05 \sigma_X \phi_0$$

Thus we can see, that T decreases approximately as:

$$\frac{1}{\sqrt{\phi^0}} \quad (\text{see section 4.3.1})$$

(iii) STABILITY AS FUNCTION OF MEAN FLUX LEVEL

We use (3) in order to determine the mean flux level influence on stability, and as a measure of stability we take the critical core height.

We cannot be sure that the parameters are unaltered for very high fluxes. Therefore, this calculus will only show, what happens if only mean flux level is varied in the equations.

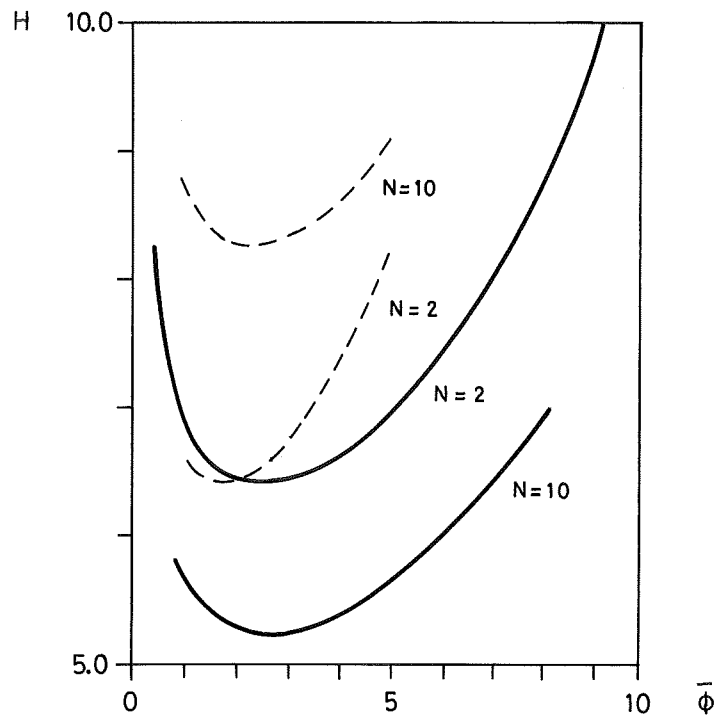


Figure 2. Critical height H (m) as function of mean flux $\bar{\phi}$ for the two point model and a multipoint model.

N = number of meshpoints.

Temp. coeff. $\alpha = -0.0514$

----- = sine flux
 _____ = flat flux

Figure 2 shows the critical height as function of mean flux.

Let us now study the asymptotic behaviour (big mean flux) of the curves:

(a) Temperature coefficient nonzero

We make a conservative estimation in (3) and neglect λ_i and λ_x for big ϕ^0 . Thus

$$\sigma_x \phi^0 \left[1 - \frac{(\gamma_x - X^0) h^2 \beta}{2 - \alpha h^2 \phi^0} \right] > 0$$

for stability. If

$$\phi^0 \geq \frac{\beta(\gamma_x - X^0)}{\alpha}$$

and $\alpha < 0$, the critical height tends to infinity.

For $\alpha = -0.0514$ (see fig. 2) we get infinite critical height for

$$\phi^0 > 13.5 = 13.5 \cdot 5.65 \cdot 10^{13} = 7.6 \cdot 10^{14} \text{ neutr./cm}^2 \text{ sec.}$$

(b) Temperature coefficient $\alpha = 0$

Now the asymptotic behaviour of (3) gives a conservative estimate:

$$\sigma_x \phi^0 [2 - (\gamma_x - X^0) h^2 \beta] > 0 \quad \text{or}$$

$$h^2 < \frac{2}{(\gamma_x - X^0) \beta} = 2.88 \quad (H^0 < 5.1 \text{ m})$$

for stability.

The dependence of the mean flux which has been shown here is later confirmed by the linear multipoint models and the non-linear transient model (see fig. 2 and section 4.3.1)

(iv) TEMPERATURE COEFFICIENT INFLUENCE ON CRITICAL HEIGHT
is shown in figure 3. This simple dependence is found in (3),
where

$$g = \frac{2}{h^2} - \alpha \phi^0 \quad (\text{see eq. 2:44})$$

The behaviour is easy to confirm with more complicated models
(see section 4.3.2)

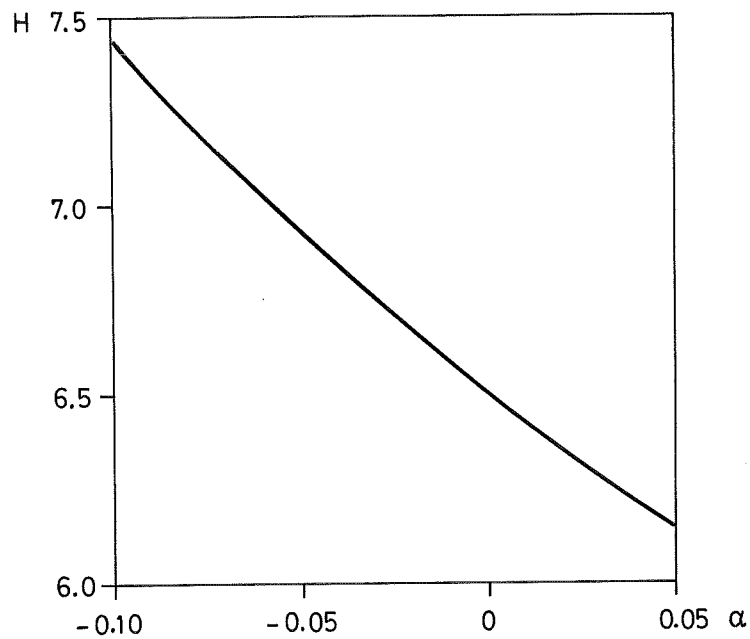


Figure 3. Critical height H (m) as function of the
temperature coefficient α for the linear
symmetric two point model.
Mean flux $\bar{\phi} = 1$

4.1.2 INFLUENCE OF ASYMMETRY OF THE FLUX

The degree of stability is influenced very much by the asymmetry of the flux. Figure 4 shows the locus of the three first eigenvalues of the system matrix A (2:52) for the homogeneous control case as function of an asymmetry measure ζ , which is defined

$$\phi_1^0 = \zeta \cdot \bar{\phi}$$

$$\phi_2^0 = (2 - \zeta)\bar{\phi}$$

The eigenvalues are calculated with program ASSXE (app. 2)

The fourth eigenvalue is always constant $s_4 = -\lambda_1$, and is neglected here. For symmetric flux ($\zeta = 1$) the flux is on the stability limit.

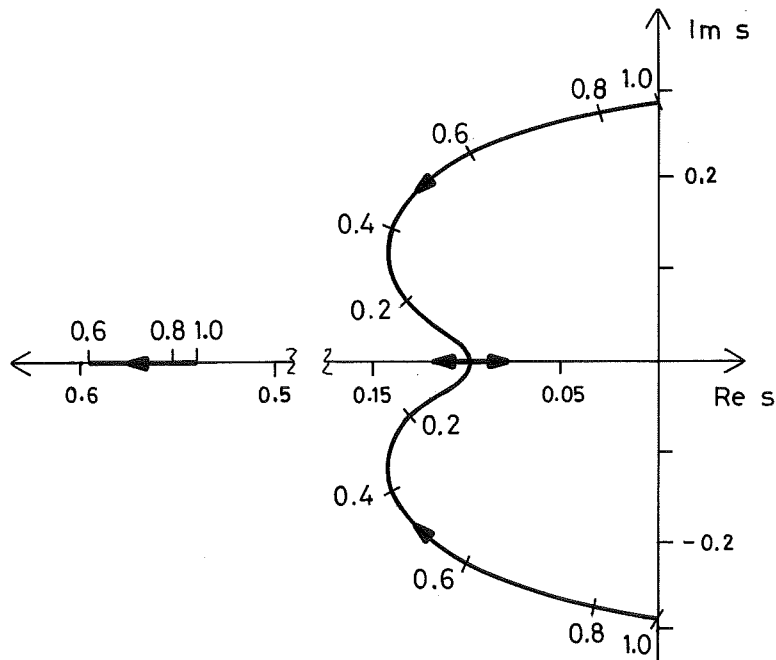


Figure 4. The locus of the three most significant eigenvalues of the linearized asymmetric two point model with homogeneous control.(2:52). The asymmetry variable ζ ($\zeta = 1$ for symmetry) is used as parameter.

Core height = 6.93 m

Temp.coeff. $\alpha = -0.0514$

Mean flux $\bar{\phi} = 1$

4.2 INFLUENCE OF THE NUMBER OF MESHPOINTS ON STABILITY CALCULATIONS

4.2.1 CRITICAL CORE HEIGHT

The critical height of the core is determined as function of N for two standardized fluxes, the flat flux and the sinusoidal flux. The control c is assumed to be homogeneous. In the flat flux case it is shown that this fact has no importance (see 2.8.2). It is also intuitive clear that the rod configuration has no influence on the linear stability for other flux forms, as the rod movement is small, for small disturbances. This is confirmed by calculations.

A program XELI (XEnon LInear model) has been written, which generates the system matrix out of (2:57) - (2:60) with the condition (2:61), which reads:

$$c_k = c \qquad k = 1, \dots, N$$

in the homogeneous case. (program listing in Appendix 2)

We use the special forms of the diffusion equation (2:59) which are calculated for the flat flux (2:79) and for the sinusoidal flux (2:86).

The program XELI then determines the critical height and the eigenvalues of A_N .

Figure 5 shows the critical height as function of the number of meshpoints for

$$\bar{\phi} = 1 \qquad (\text{see (2:65) and (2:87)})$$

The figure shows the well-known fact, that the critical height increases with the form factor.

The critical height converges asymptotically to a certain value. We want to examine if it is possible to extrapolate to the right critical height (infinite number of meshpoints) out of simple models. We will give a few numerical examples below.

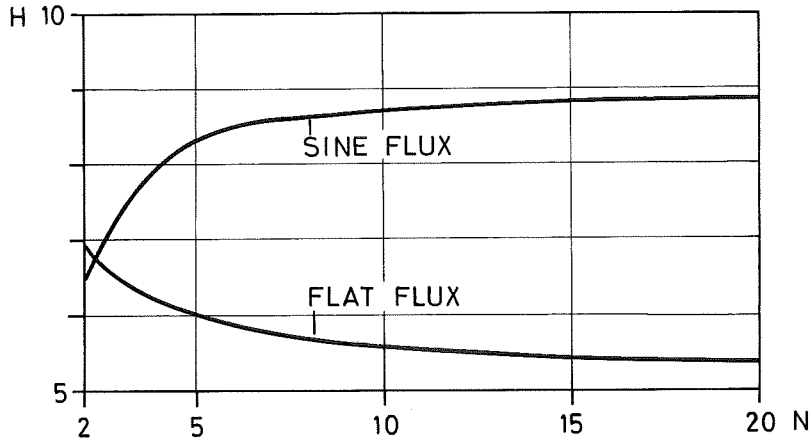


Figure 5. Critical core height $H(m)$ for multipoint models as function of the number of meshpoints of the core (N) for two different symmetric flux shapes.

Mean flux $\bar{\phi} = 1$

Temp. coeff. $\alpha = -0.0514$

(i) FLAT FLUX

Assume the curve in figure 5 has the form:

$$H(N) = H(\infty) + ae^{-b(N-2)} \quad (7)$$

where a , b , and $H(\infty)$ are parameters to be determined. From $N = 2, 3, 4$ we get:

$$H(\infty) = 5.55 \text{ m}$$

$N = 20$ inserted gives $H(20) = 5.55 \text{ m}$.

The right value of $H(20)$ is 5.38 m , why the error is 3.2% .

$N = 5, 6, 7$ gives $H(\infty) = 5.52 \text{ m}$

Extrapolation to $H(20) = 5.53 \text{ m}$

Error = 2.8%

$N = 8, 9, 10$ gives $H(\infty) = 5.40 \text{ m}$

Extrapolation to $H(20) = 5.43 \text{ m}$

Error = 0.9%

$N = 11, 12, 13$ gives $H(\infty) = 5.33 \text{ m}$

Extrapolation to $H(20) = 5.39 \text{ m}$

Error < 0.2%

The TRAXEN program calculates the critical height for flat flux [15] to 5.36 m, 0.02 m from the linearized model, where $N = 20$ in both cases.

(ii) SINUSOIDAL FLUX

We extrapolate three points to an asymptotic value here as in (7).

Exponential extrapolation from

$N = 2, 3$ and 4 gives $H(\infty) = 8.68$ m
and an estimation of $H(20) = 8.68$ m

$N = 5, 6, 7$ gives $H(\infty) = 8.83$ m and
 $N = 8, 9, 10$ gives $H(\infty) = 8.89$ m

from which $H(20)$ is calculated to 8.89 m.

The TRAXEN program [15] estimates the critical height for 20 meshpoints to be about 8.89 m for the sinusoidal flux. This shows that we can estimate the critical height in a conservative direction within 2.4% by extrapolation from $N = 2, 3, 4$.

4.2.2 THE EIGENVALUES FOR SOME DIFFERENT NUMBERS OF NODE POINTS

We show the eigenvalues of the system matrix at the critical height as function of the number of meshpoints. The system matrix is of order $2N \times 2N$ (eq. 2:57, 58, 65). Two eigenvalues are constant (2:64) why we show only $2 * (N-1)$ eigenvalues in the table.

In table 1 is shown the eigenvalues of the flat flux. The period time is, as we can see, estimated very accurately already with the two point model ($N = 2$) and is found to be:

$$T = \frac{2\pi}{0.26389} = 23.81 \text{ hours}$$

for all cases.

Table 1
 Contd.

N	H _{crit} (m)	Real part	Imag. part
		- 0.11095	0
		- 0.11267	0
		- 0.11565	0
		- 0.12163	0
		- 0.13746	0
		- 0.23550	± 0.07478
		- 0.43120	0
		- 0.48207	0
		- 0.50441	0
		- 0.51631	0
		- 0.52341	0
		- 0.52797	0
		- 0.53107	0
		- 0.53326	0
		- 0.53485	0
		- 0.53604	0
		- 0.53693	0
		- 0.53762	0
		- 0.53813	0
		- 0.53852	0
		- 0.53880	0
		- 0.53899	0
		- 0.53910	0

For the sinusoidal flux we get the eigenvalues shown in table 2. We can see directly that the estimation of the period for the oscillations increases significantly when the number of meshpoints is increased from 2 to 10. Already three space points is a far better approximation than two points for this flux.

Table 2

Eigenvalues for sinusoidal flux at critical height for different number (N) of core node points.

Mean flux $\bar{\phi} = 1$

Temp. coeff. $\alpha = -0.0514$

N	H _{crit} (m)	Real part	Imag. part	T(hrs)
2	6.568	0.00000	±0.30555	20.56
		-0.77950	0	
		-0.10600	0	
3	7.577	-0.00001	±0.27869	22.55
		-0.10600	0	
		-0.18615	±0.22326	
		-0.72128	0	
4	8.105	0.00000	±0.27383	22.95
		-0.10600	0	
		-0.18183	±0.19005	
		-0.25651	±0.11402	
		-0.69896	0	
5	8.385	0.00000	±0.27282	23.03
		-0.10600	0	
		-0.18323	±0.17251	
		-0.18810	0	
		-0.23431	±0.09106	
		-0.42473	0	
		-0.68871	0	
10	8.807	0.00000	±0.27212	23.09
		-0.10600	0	
		-0.12070	0	
		-0.12226	0	

forts.

N	H _{crit} (m)	Real part	Imag. part	T(hrs)
		-0.12490	0	
		-0.12943	0	
		-0.13800	0	
		-0.15877	0	
		-0.19331	± 0.14763	
		-0.19505	± 0.05651	
		-0.25615	0	
		-0.38003	0	
		-0.47547	0	
		-0.56196	0	
		-0.63661	0	
		-0.67486	0	
		-0.69978	0	

4.3 COMPARISON BETWEEN DIFFERENT MODELS OF INFLUENCE OF CERTAIN CORE PARAMETERS

4.3.1 DEPENDENCE OF MEAN FLUX LEVEL

Even for more complicated models we can establish the result from the two point model (section 4.1.1). The critical height as function of the mean flux level is shown in figure 2 for a 10 point model with flat and with sinusoidal flux. The curves for N=2 and N = 10 are quite parallel.

With the TRAXEN program a quite similar result is shown for a flattened sinusoidal flux [15] and small disturbances.

The oscillation period at critical height for different flux levels is shown in table 3 for the two point, the ten point and the non-linear TRAXEN models.

Table 3

Oscillation period (hrs) at critical height for different flux shapes and mean flux levels ($\alpha = - 0.0514$)

$\bar{\phi}$	Flat flux ($\psi = 1.0$)		Sinusoidal flux ($\psi \rightarrow \frac{\pi}{2} = 1.57$)		Flat sinusoidal flux $\psi = 1.35$
	N = 2	N = 10	N = 2	N = 10	TRAXEN (N = 20)
1	23.81	23.81	20.56	23.09	24.5
2	18.32	18.32	15.38	18.05	-
3	15.38	15.38	12.80	15.35	-
4	13.51	13.51	11.19	13.63	-
5	12.19	12.19	10.06	12.42	13.0

The table shows, that the period decreases, when the mean flux increases from 1 to 5, and the decrease is

- 51% for the flat flux (N = 2 and 10)
- 49% " " sinusoidal flux (N = 2)
- 54% " " " " (N = 10)
- 53% " " TRAXEN flux (N = 20)

4.3.2 DEPENDENCE OF TEMPERATURE COEFFICIENT

Fig. 3 shows the critical height as function of α for the two point model. Even for the multipoint models the critical height decreases for increasing temperature coefficient. As table 4 shows, the rate of decrease of critical height is very accurately determined for flat flux with the two point model, while we need three node points to get relatively good accuracy for the sine flux.

Critical height H_0 (m) as function of temperature coefficient at different number of core meshpoints (N).

Mean flux = 1

$$K = \frac{\Delta H}{H_0} \cdot \frac{\alpha}{\Delta \alpha}$$

Flat flux			
N	H_0 ($\alpha = -0.0514$)	H_0 ($\alpha = 0$)	K
2	6.929	6.499	0.0622
3	6.533	6.126	0.0623
4	6.250	5.861	0.0622
8	5.735	5.378	0.0622
10	5.621	5.271	0.0622
Sinusoidal flux			
2	6.568	6.034	0.081
3	7.577	7.057	0.069
4	8.105	7.547	0.069
8	8.723	8.124	0.069
10	8.807	8.204	0.068

4.3.3 FLUX FORM INFLUENCE

(i) ASYMMETRY

In 4.1.2 we showed that stability could be better for an asymmetric flux than for a symmetric one. Exactly the same thing is shown with the TRAXEN model and small disturbances, where the convergence of the transients increased for a slight asymmetric flat flux [15].

(ii) FORM FACTOR IN SYMMETRIC FLUX

It is a well-known fact that stability increases for a higher form factor (see figure 5). However, for the two point model the result is opposite. From the discussion in preceding sections we can conclude, that two points give a very good information of flat flux, but not so good for sine flux, where three points seems to be far much better (see the tables 2 - 4). This can be intuitively understood by the fact that two points cannot represent the curvature very good, but three points seem to be rather good, because the midpoint can represent the top of the sine curve.

The critical height as function of form factor Ψ has been calculated with three different models, shown in table 5. The different flux shapes are shown in figure 6.

Table 5

Critical height H (m) for different form factors Ψ calculated with different models. ($\bar{\phi} = 1, \alpha = -0.0514$)

Ψ	TRAXEN (N=20)	Modal expansion (Clean reactor)	Linear model (§ 2.8) N=20
1.0	5.36	-	5.38
1.14	5.15	5.2	-
1.35	7.5	7.6	-
1.57	8.89	-	8.89

The modal expansion model is presented by Norinder [13]. We can directly see, that the form factor cannot uniquely determine the critical height. The "ditch" flux has a lower stability than a flat flux. The two halves of the core are less coupled together for a ditch flux, which may explain the lower stability.

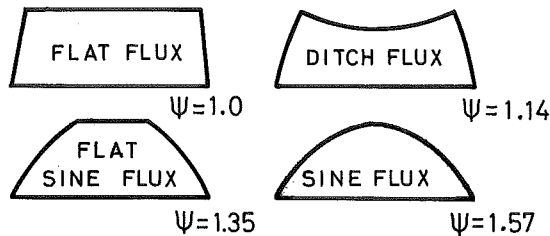


Figure 6. Different flux shapes used in the calculations.

5. CHARACTER OF THE SOLUTIONS OF THE NONLINEAR MODELS

The nonlinear trajectories for the two point model have been studied by digital simulations in 5.1. As the two point model is very simple we can quickly study a big number of trajectories. The most interesting ones can then be compared to more complex models, and we have used the TRAXEN nonlinear model in order to compare the results in 5.2.

The most interesting nonlinear terms are the control term and the temperature coefficient. It is shown that periodic solutions can appear in several cases. The nature of the limit cycle is strongly dependent on the control term as well as the temperature coefficient.

With rod control both unstable and stable periodic solutions may appear. With homogeneous control, however, there are only stable periodic solutions.

All the different types of nonlinear behaviour of the two point model have been verified by digital simulation of the TRAXEN model in section 5.2. There is, however, some important quantitative differences of the behaviour with rod control. The amplitudes of the unstable periodic solutions are smaller, while the amplitude of the stable ones are bigger than those of the TRAXEN model. A physical interpretation of the result is given.

5.1 THE TWO POINT MODEL

5.1.1 QUALITATIVE DISCUSSION OF INFLUENCE OF NONLINEAR TERMS

A Fortran program XETRA (XEnon TRAnsient) has been written (appendix 2) in order to solve the nonlinear system, equations (2:37 - 40) of the two point symmetric model with $\phi^0 = 1$ (flat flux). There are three important nonlinear terms involved in the equations. As proved in section 2.7.3 the type of control has no influence on stability for the linear symmetric flux, but it is an essential nonlinear factor for stability in the large. The two cases rod control and homogeneous control are treated separately in the following sections. The direction of the disturbance has a big influence on the character of the trajectory in the rod control, which is verified by simulations.

The next important term is the temperature coefficient α , which has influence on the eigenvalues of the linear system as well as the nonlinear character of the trajectories. A negative α has a stabilizing effect on the system. The quadratic term in the xenon equations (2:37, 39) always gives a positive contribution to the xenon increment derivative. This depends on the fact, that the increments of xenon and neutron flux in a space point have approximately opposite sign, which can be realized by simple analysis, see (2:48, 50) and (2:44, 46). Simulations have verified this result, [15]. Thus, the term $-\sigma \xi \varphi$ in (2:37, 39) is positive almost always.

5.1.2 PERIODIC SOLUTIONS WITH ROD CONTROL

The dynamic system is described by (2:37 - 40) with (2:42 - 43) inserted.

Depending on the eigenvalues of the linear approximation and on the disturbances we get different types of solutions.

As mentioned in previous section, the parameter α determines the character of the nonlinear solutions. The state variable x_4 does not affect the nonlinear behaviour at all (2:40), why it is not interesting to show it in the diagrams. x_4 converges to zero, which means that iodine is varying in opposite direction in the two space points.

Figure 1 shows the qualitative appearance of the phase plane of the solutions for different temperature coefficients and core heights (see also figure 2:3).

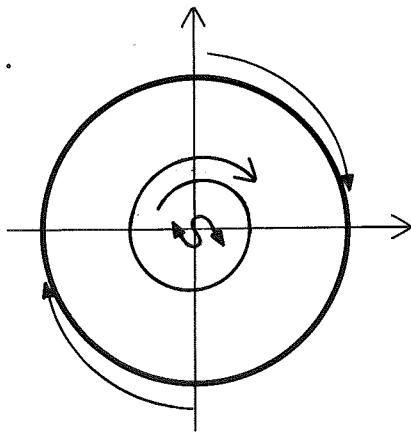
Directly from figure 1 we can conclude some important features of the solutions

(i) $\alpha = -0.02$

When increasing the core height the eigenvalues of the linear approximation move towards right and the influence of the nonlinear terms will change. At the smallest core height (1:E) it is impossible to get unstable solutions even for very big disturbances. When the size grows it is possible to get unstable solutions for reasonable disturbances; thus we get an unstable limit cycle (1:D). Figure 2 shows the unstable limit cycle for

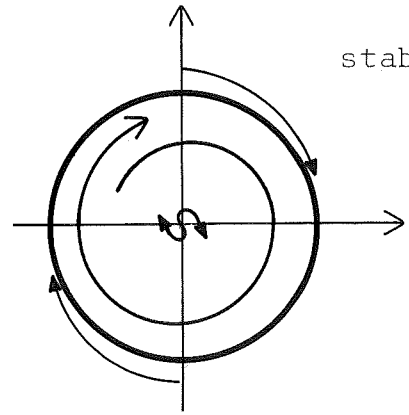
A

stable l.c.


 $\text{Re } s \gg 0$
 unstable node

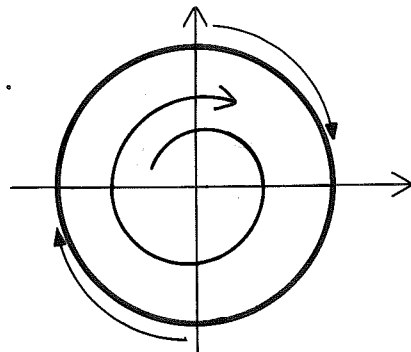
F

stable l.c.



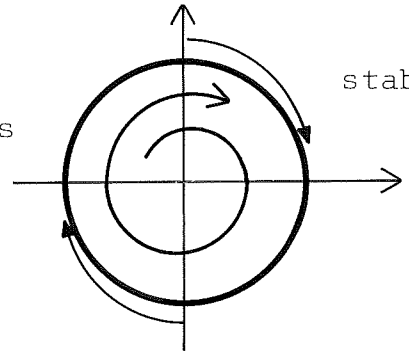
B

stable l.c.


 $\text{Re } s > 0$
 unstable focus

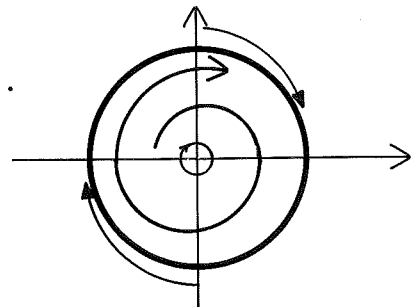
G

stable l.c.



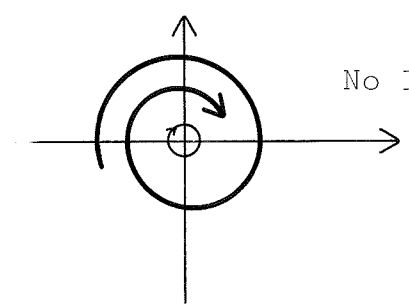
C

stable l.c.

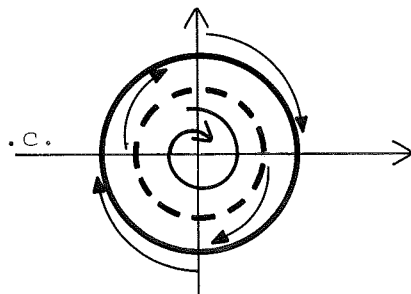

 $\text{Re } s = 0$
 center

H

No l.c.

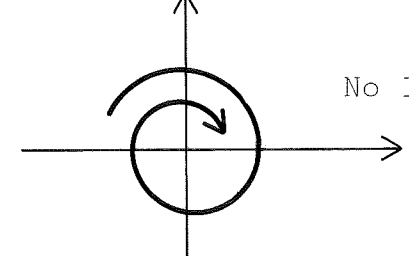


D

stable and
unstable l.c.
 $\text{Re } s < 0$
 stable focus

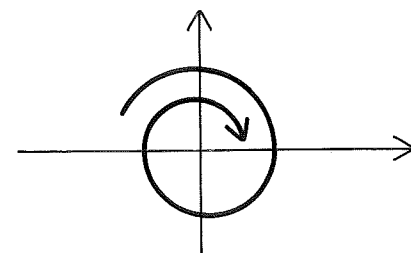
J

No l.c.



E

No l.c.


 $\text{Re } s \ll 0$
 stable focus or
 stable node

K

No l.c.

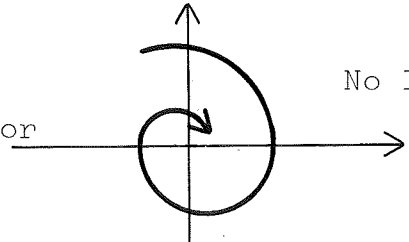


Figure 1

Symbolic phase planes of the nonlinear two point model of a symmetric flux with rod control at different temperature coefficients α and core heights.

Mean flux level $\bar{\phi} = 1.0$

$\text{Re } s$ = real part of biggest eigenvalue, at the singular point.

$H = 6.62$ m, 0.04 m below the critical height. We see the projection in the $x_1 - x_3$ plane. The period time is near 24 h.

A disturbance of

$$x = \begin{pmatrix} 0.25 \\ 0 \\ 0 \\ 0 \end{pmatrix}$$

is enough to get an unstable solution.

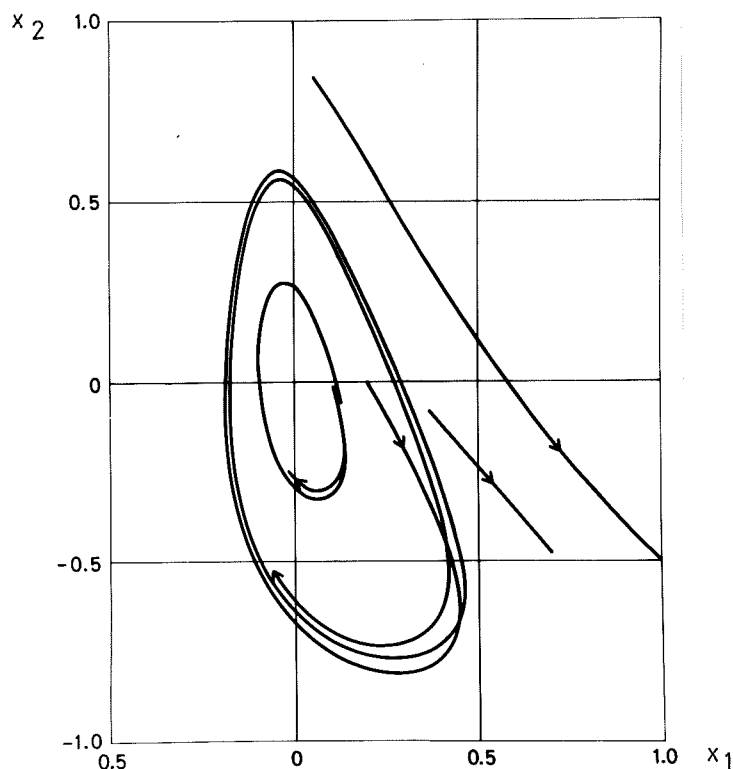


Figure 2. Projection of the state space into the x_1-x_2 plane of the nonlinear two point reactor model with rod control. Origo is a stable focus. Solutions near origo converges asymptotically while trajectories from large disturbances outside an unstable limit cycle diverge towards a stable periodic solution (not shown in the fig.)

$x_1 = \xi_1 =$ xenon deviation in space point 1

$x_2 = \eta_1 =$ iodine deviation in space point 1

$\bar{\phi} = 1.0$ $\alpha = -0.02$ $H = 6.62$ m ($H_{crit} = 6.66$ m)

(Compare figure 1:D)

The amplitude of this limit cycle decreases as the core height increases and it approaches zero at the critical height (1:C). There is even a stable periodic solution, which appears already below the critical height (1:D). The amplitude of this periodic solution increases with the core height. Already below the critical height the stable limit cycle amplitude is unrealistically big.

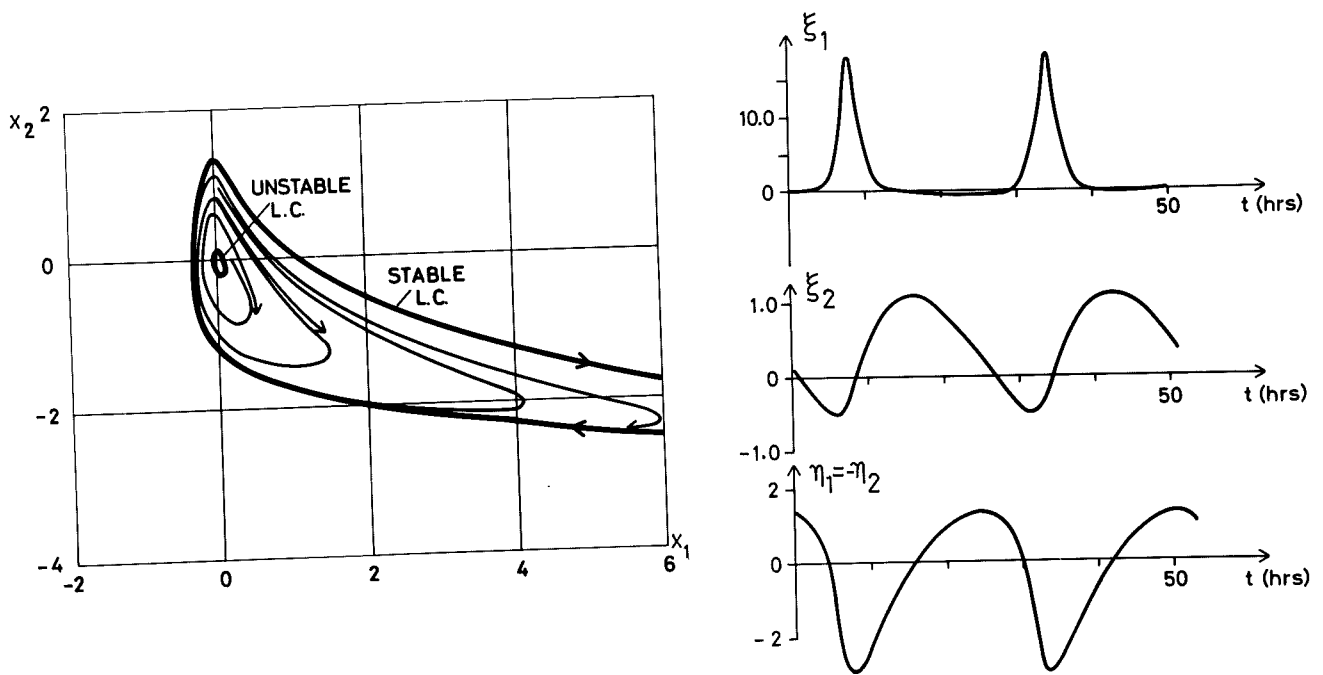


Figure 3A

Projection of the state space into the $x_1 - x_2$ plane of the nonlinear two point reactor model with rod control. Origo is a stable focus. Solutions near origo are asymptotically stable and are not shown in figure. At the outside of the unstable limit cycle, the solutions are diverging towards a stable limit cycle, which is strongly asymmetric.

$$\xi_1 = x_1 = \text{xenon deviation in space point 1}$$

$$\xi_2 = x_3 - x_1 = \text{xenon deviation in space point 2}$$

$$\eta_1 = x_2 = \text{iodine deviation in space point 1}$$

$$\bar{\phi} = 1.0 \quad \alpha = -0.02 \quad H = 6.64 \text{ m} \quad (H_{\text{crit}} = 6.66 \text{ m})$$

(Compare figure 1:D)

Figure 3B

The limit cycle as function of time.

Figure 3 shows the trajectories for a core $H = 6.64$ m, 0.02 m below the critical height (compare fig. 1:D). The unstable limit cycle is very small. The unstable trajectories diverge toward a stable limit cycle.

The extreme values are

$$x = \begin{pmatrix} 18.06 \\ 17.74 \\ -3.00 \\ 0 \end{pmatrix}$$

and the period time 25.5 hrs. Thus the limit cycle is so big that it has to be avoided.

We also observe the very strong asymmetry of the trajectories. This depends on the rod configuration, and is discussed more in section 5.2.1.

(ii) $\alpha = -0.05$

No unstable limit cycle will occur in this case and it is interesting to study what happens at the critical height when α varies.

For a decreasing α , from -0.02 to -0.05 , the critical height increases and the influence of the nonlinear terms changes. For big disturbances the solutions are unstable for $\alpha = -0.02$ and stable for $\alpha = -0.05$ at the two different critical heights.

The stable limit cycle decreases to a zero amplitude for core heights below the critical heights when α decreases from -0.02 to -0.05 (see fig. 1:C, H and 1:D,J). For core heights bigger than the critical ones the stable limit cycle decreases to a smaller value (compare fig. 1:A, F and 1:B, G).

When α is constant the amplitude of the limit cycle increases for increasing core height.

The stable limit cycle at $H = 6.97$ m and $\alpha = -0.05$ (compare fig. 1:G), 5 cm over the critical height, is much smaller than the former limit cycle in fig. 3 (or fig. 1:B, C, D) and is shown in figure 4:A - D. The period time is found to be 24.2 h.

The asymmetry of the periodic solution is not so big here as in the former case (figure 3), because the temperature coefficient damps the big amplitudes very strongly (compare section 5.2.1)

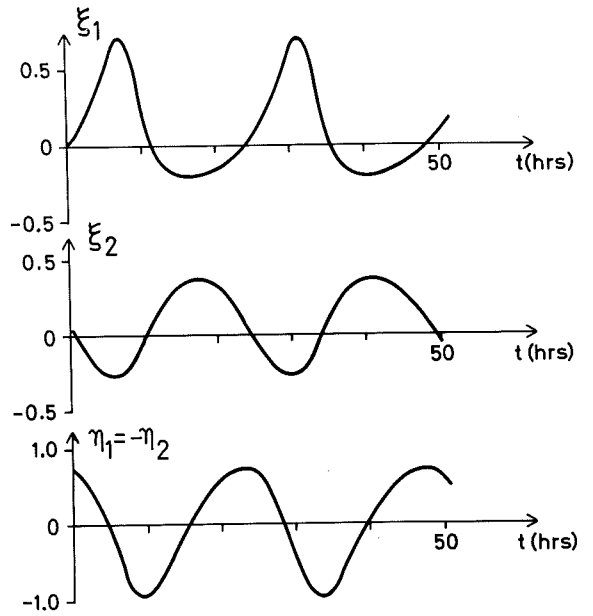
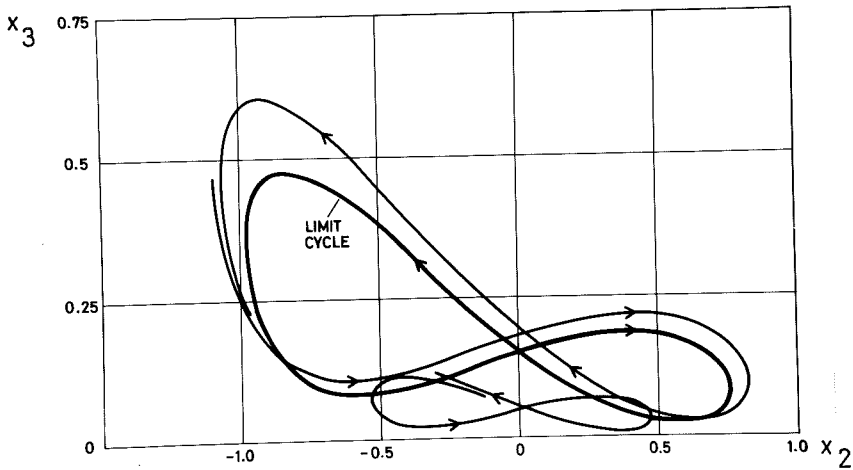
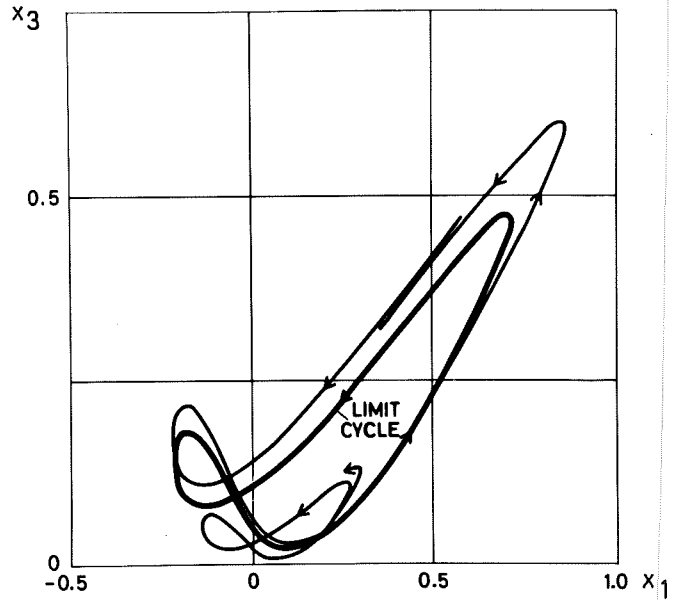
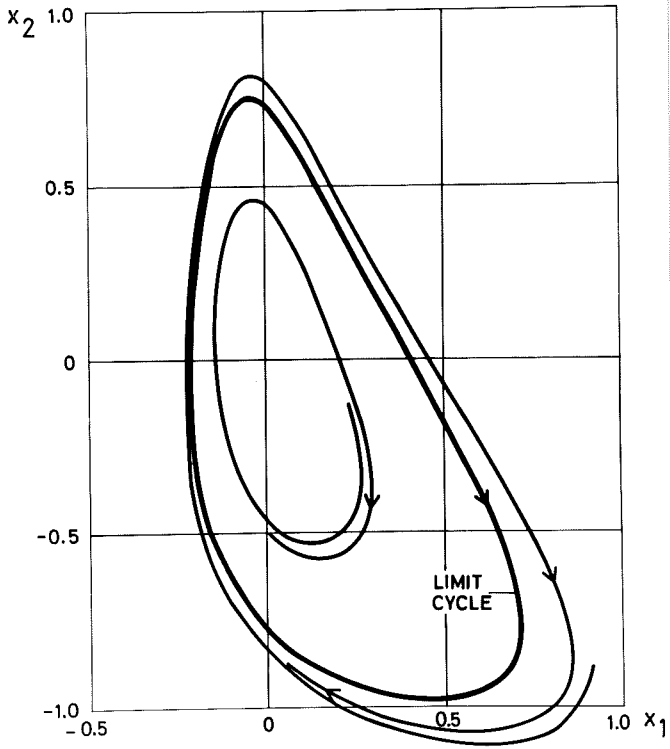


Figure 4 A-C.

Projection of the state space into three planes of the nonlinear two point model with rod control. The singular point is unstable and the trajectories from origo diverges towards a stable limit cycle.

$x_1 = \xi_1$ = xenon deviation in space point 1

$x_2 = \eta_1$ = iodine deviation in space point 1

$x_3 = \xi_1 + \xi_2$ = sum of xenon deviations

$x_4 = \eta_1 + \eta_2$ = sum of iodine deviations

$\bar{\phi} = 1.0$ $\alpha = -0.05$ $H = 6.97$ m ($H_{crit} = 6.92$ m)

(Compare figure 1:G)

Figure 4 D.

The limit cycle as function of time.

5.1.3 PERIODIC SOLUTIONS WITH HOMOGENEOUS CONTROL

The description of the dynamic system is found in (2:37-40) with (2:46, 47) inserted. As in the rod control case, the equations have been simulated on a digital computer. The flux equation (2:46) is solved with the Newton - Raphson method.

As proved in 2.7.3 the control arrangement has no influence on the linear stability, why the critical heights are unaltered, compared with the rod control. Figure 5 shows the type of solutions in the homogeneous control case.

There are some important differences to the control rod case. First we have no unstable limit cycle and then the amplitude of the stable limit cycle is much smaller and more regular. All the time $x_3 = \xi_1 + \xi_2$ is small, which means, that the oscillation of xenon and iodine in point one has a phase just the opposite of point two.

Figure 6 shows the stable limit cycle related to figure 5:B, namely $H = 6.68$ m, 2 cm over critical height. Compared to the rod case (fig. 3) the amplitude is very moderate and the curve rather regular. Period time is just below 24 hrs.

The amplitude of the stable limit cycle grows rather fast when core height increases. Figure 7 shows $\alpha = -0.05$ and $H = 6.94$ m, 2 cm over the critical height. For $H = 6.97$ m the limit cycle amplitude has grown another 67%, while the form of the curve is quite the same. The period is just about 24 hrs.

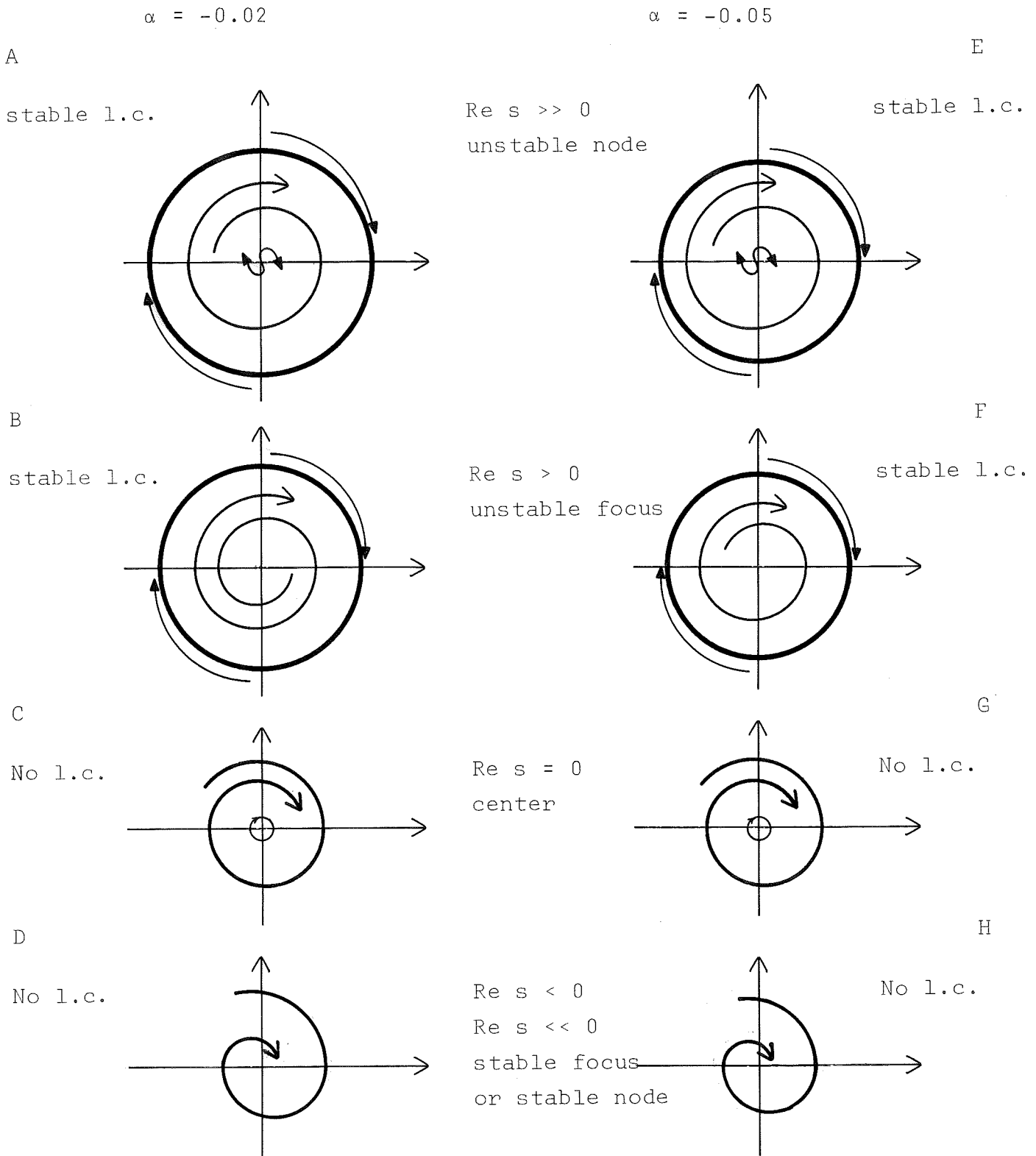


Figure 5 Symbolic phase planes of the nonlinear two point model of a symmetric flux with homogeneous control at different temperature coefficients α and core heights H .
 Mean flux level $\bar{\phi} = 1$
 Re s = real part of biggest eigenvalue at the singular point.

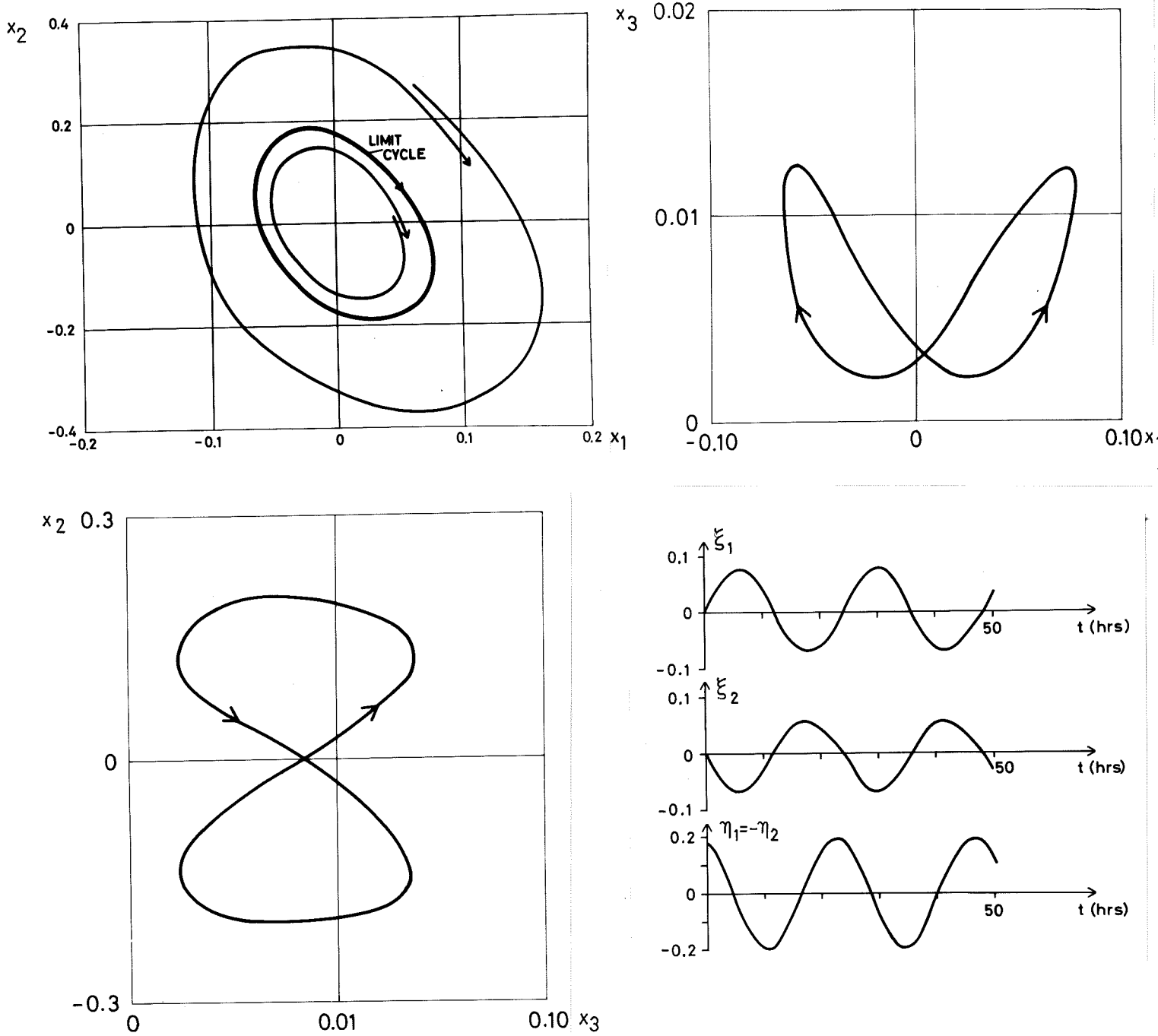


Figure 6 A-C. Projection of the state space into the three planes of the nonlinear two point model with homogeneous control. The singular point is unstable and the trajectories from origo diverges towards a stable limit cycle. (Compare fig.3)

- $x_1 = \xi_1 =$ xenon deviation in space point 1
- $x_2 = \eta_1 =$ iodine deviation in space point 1
- $x_3 = \xi_1 + \xi_2 =$ sum of xenon deviations
- $x_4 = \eta_1 + \eta_2 =$ sum of iodine deviations

$\bar{\phi} = 1.0 \quad \alpha = -0.02 \quad H = 6.68 \text{ m} \quad (H_{\text{crit}} = 6.66 \text{ m})$

(Compare fig. 5:B)

Figure 6 D. The limit cycle as function of time.

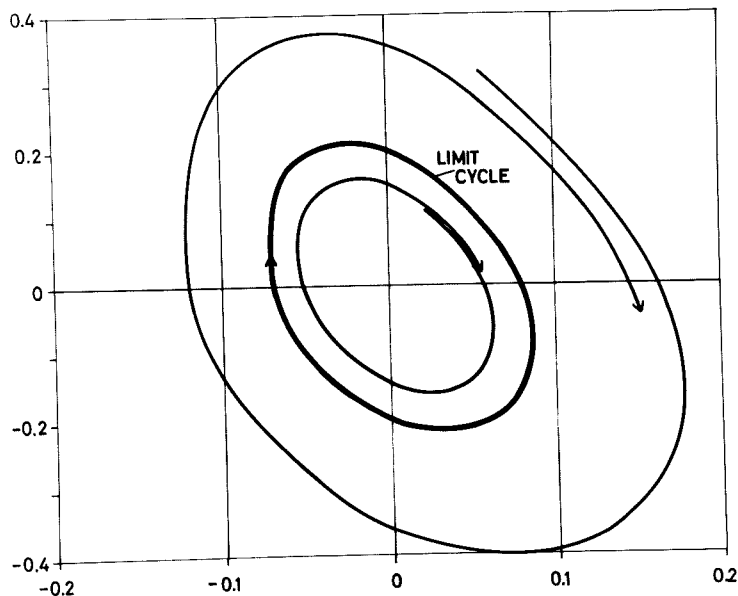


Figure 7. Projection of the state space into the $x_1 - x_2$ plane of the nonlinear two point model with homogeneous control. The singular point is unstable and a stable limit cycle appears. (Compare fig. 4 and 6)

$x_1 = \xi_1 =$ deviation of xenon in point 1

$x_2 = \eta_1 =$ deviation of iodine in point 1

$\bar{\phi} = 1.0 \quad \alpha = -0.05 \quad H = 6.94 \text{ m} \quad (H_{\text{crit}} = 6.92 \text{ m})$

(Compare fig. 5:F)

Even for positive values of α we get a stable periodic solution for a core height over the critical height. This result should be compared to [1], where nonoscillating unstable trajectories were found for positive α . See also [15], chapter 5.

5.2 COMPARISONS BETWEEN THE TWO POINT MODEL AND THE NONLINEAR TRANSIENT STUDIES WITH TRAXEN

5.2.1 ROD CONTROL

The character of nonlinear solutions of the two point model has been completely verified by digital simulation of the TRAXEN model of a flat flux. All the stable period solutions shown in fig. 1 are verified, as well as the unstable limit cycle. Quantitatively there are some important differences which must be stressed.

The first interesting quantity is the amplitude of the limit cycles. In order to be able to compare the calculations, we should use quite the same core parameters. As the critical heights of the two models differ by 28% (4.2.1), we can only compare the order of magnitude. The period of the limit cycles, however, are quite the same. Generally the two point model has smaller amplitudes of the unstable limit cycles and bigger amplitudes of the stable limit cycles. The latter fact is specially clear when α is more positive as the stabilizing effect of α is smaller.

The most important cause to the difference is the rod configuration. In the two point case the "rod" is acting in one point, which means that it is uniformly "distributed" along half the core. As the oscillations are mainly described as first overtone oscillations, this configuration has a maximum damping or amplifying effect on the oscillation amplitude, and fig. 3 and 4 show clearly that the transient is damped once and amplified once during a cycle depending on the rod.

When the symmetric flux is disturbed, the absorption in the core must be increased, which will cause the flux in the "rod point" to decrease. Now, if the first disturbance has a direction which is the same as the absorption effect, the rod causes a strong amplification. Thus it is easier to get unstable solutions and the stable solutions get a bigger amplitude.

In the complex transient model the rod arrangement is different as the rod is inserted and withdrawn during an oscillation. The amplitude of this movement depends on the absorption along the rod. The amplifying or damping effect gets smaller and even the amplitudes of the stable solutions. It is also more difficult to get unstable limit cycles with the TRAXEN model of the same reasons. However, for ditch fluxes (fig.4:6) the unstable limit cycles are verified. A ditch flux which was stable for small disturbances and some 10 cm below the critical height was disturbed by 100 pcm moved from upper to lower core. This disturbance caused unstable oscillations, see [15].

In order to get a rod configuration which is more like the two point model we must use a rod which is always inserted to half the core and has a variable absorption. The rod configuration problem is discussed in detail in [15], chapter 4.2.

5.2.2 HOMOGENEOUS CONTROL

Even here all the standard cases shown in figure 5 are verified by the TRAXEN model. The amplitudes of the periodic solutions are now of the same order of magnitude in the two models, which is quite natural, as no rod can influence on the result.

Fig. 8 gives one numerical example of a flat flux, $H = 5.40$ m, $\alpha = -0.0514$, which is 4 cm over the critical height. If 1% reactivity is moved from one half of the core to the other we get stable solutions, while small disturbances cause unstable solutions.

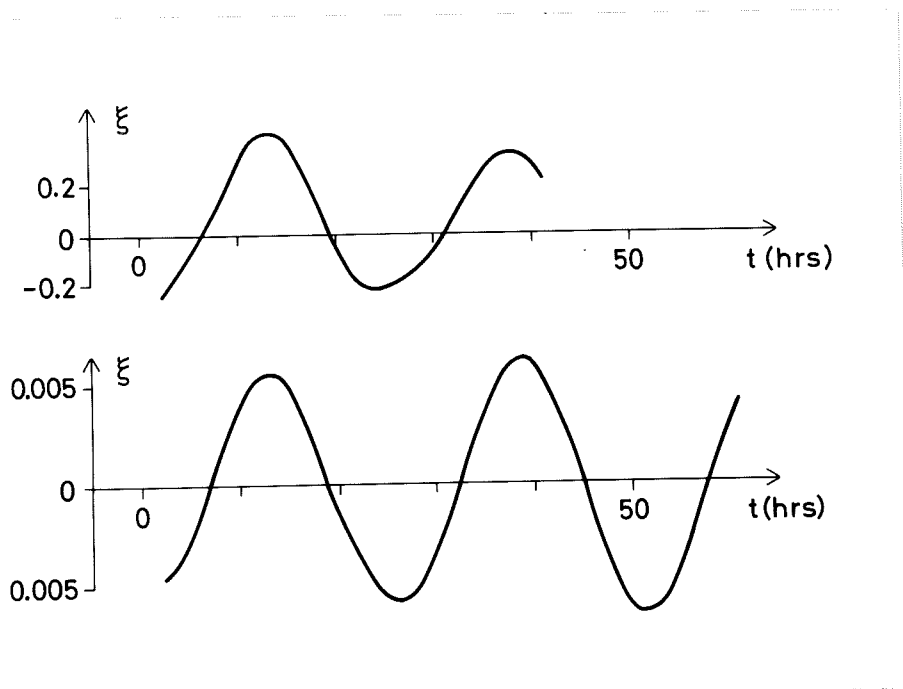


Figure 8. A local trajectory of xenon deviation at the core point $z/H = 0.95$ calculated with the TRAXEN digital program of a 20-point nonlinear reactor model with homogeneous control. Flux shape is symmetric flat (see fig. 4:6)

$$\bar{\phi} = 1.0$$

$$\alpha = -0.0514$$

$$H = 5.40 \text{ m } (H_{\text{crit}} = 5.36 \text{ m})$$

The disturbance consists of r pcm reactivity moved from one core half to the other during 2 hours. Large disturbance trajectories converge and small disturbance trajectories diverge to a stable limit cycle.

ACKNOWLEDGEMENT

The author wishes to express his appreciation to professor K.J. Åström for stimulating discussions and constructive criticism. The subroutines from the program library are written by K. Mårtensson. The author also wishes to acknowledge Mrs. G. Christensen and Miss L. Jönsson who typed the manuscript and Mrs. B. Tell who drew the figures.

REFERENCES

- {1} J. Chernick, G. Lellouche and W. Wollman: The Effect of Temperature on Xenon Instability, Nucl.Sci.Eng. 10, 120 - 131 (1961)
- {2} S. Glasstone and M.C. Edlund: The Elements of Nuclear Reactor Theory, Van Nostrand, Princeton, New Jersey, 1952
- {3} E.P. Gyftopoulos: Applications of Geometric Theory to Nonlinear Reactor Dynamics, Nucl.Sci.Eng., 10, 254-268 (1961)
- {4} R.R. Haefner: Flux Oscillations Caused by Xenon Instability, Nucl.Sci.Technol., 2(3), 291 (1956)
- {5} A.F. Henry and J.G. Germann: Oscillations in the Power Distribution within a Reactor, Nucl.Sci.Eng., 2, 469 - 480 (1957)
- {6} R.J. Hooper, R.A. Rydin, and W.M. Stacey: Verification of a Xenon Spatial Stability Criterion, Trans.Am.Nucl. Soc., 11, 227 (1968)
- {7} S. Kaplan: The Property of Finality and the Analysis of Problems in Reactor Space-Time Kinetics by Various Modal Expansions, Nucl.Sci.Eng., 9, 357 (1961)
- {8} S. Kaplan, A.F. Henry, S.G. Margolis and J.J. Taylor: Space-Time Reactor Dynamics, Third UN Int.Conf. on the Peaceful Uses of Atomic En., Geneva, 1964, A/Conf. 28/P271
- {9} S. Kaplan and J.B. Yasinsky: Natural Modes of the Xenon Problem with Flow Feedback - An Example, Nucl.Sci. Eng., 25, 430 - 438 (1966)
- {10} S. Kaplan: Natural Modes of the Xenon Problem with Temperature and Control Feedback, Bettis Atomic Power Lab., WAPD-TM-695, May, 1967
- {11} J.H. Leonard: Nuclear Behaviour of the Shippingport Reactor through Three Seeds, Trans.Am.Nucl.Soc., 5(1), 136 (1962)

- {12} Marviken Power Station, design Status Report, AB Atomenergi S-353, 1966, Sweden (Not for publication)
- {13} O. Norinder: Flux-shape Eigenfunction Tables for Two-Zone Slabs, AB Atomenergi, Sweden, Report RFR-231 (1963)
- {14} M.J. O'Boyle: Control of Xenon Instabilities in Large PWR's Quarterly Progress Reports, WCAP-3680-1, 2, 3, 4 (1966,1967), Westinghouse El.Corp., Pittsburgh, Penn.
- {15} G. Olsson: Digital Simulation of Axial Xenon Instability in Power Reactors, Report 6911, Division of Automatic Control, Lunds Inst.of Techn., Lund, 1969
- {16} C.G. Poncelet and A.M. Christie: The Effect of a Finite Time-Step Length on Calculated Spatial Xenon Stability Characteristics in Large PWR's, Trans.Am.Nucl. Soc., 10, 571 (1967)
- {17} D. Randall and D. S. St.John: Xenon Spatial Oscillations, Nucleonics, 16(3), 82 - 86 (1958)
- {18} W.T. Sha: Stability in the Large of Xenon Oscillations, Trans.Am.Nucl.Soc. 10, 572 (1967)
- {19} J.W. Simpson and H.G. Rickover: Shippingport Atomic Power Station (PWR), Nucleonics 16(9), 72 (1958)
- {20} H.B. Smets: The Effect of Burnable Fission Products in Power Reactor Kinetics, Nucl.Sci.Eng., 11; 133-141 (1961)
- {21} W.M. Stacey Jr: A Numerical Study of Xenon-Power Spatial Oscillations (KAPL), Trans.Am.Nucl.Soc., 11, 226 (1968)
- {22} W.M. Stacey Jr: Optimal Control of Xenon-Power Spatial Transients, Nucl.Sci.Eng., 33, 162 - 168 (1968)
- {23} A.G. Ward: The Problem of Flux Instability in Large Power Reactors, Canadian Report CRRP-657 (1956)
- {24} D.M. Wiberg: Optimal Control of Nuclear Reactor Systems. In "Advances in Control Systems", edited by C.T. Leondes, vol.5, Academic Press, New York, 1967

APPENDIX 1

DEFINITION OF SYMBOLS AND THEIR NUMERICAL VALUES

Symbol	First def. in equation	Explanation	Numerical value
A	2:49,52,53,54, 64	System matrix	
$B^2(z,t)$	2:1	Material buckling	
$(B^2)^*(z)$	2:10	Material buckling, equilibrium value	
$c(z,t)$	2:10	Absorbtion term	
$D(z,t)$	2:1	Absolute diffusion	
$E(z,t)$	2:1	Relative diffusion	
G	2:73	Matrix NxN	
g, g_1, g_2	2:22,23,36, 44		
H	2:4	Extrapolated core height (m)	
h	2:12	Distance between two node points; $h = \frac{H}{N+1}$	
H_{crit}		Critical core height	
$I(z,t)$	2:2	Iodine concentration, measured with the xenon equilibrium concentration at infinite flux as basis	
$I^0(z)$	2:7	Equilibrium value of iodine concentration	
$n(z,t)$	2:7	$I(z,t) - I^0(z)$	
$K(z)$	2:6	weight function in expression for total power	
M^2		Migration area	440 cm ²
N	2:12	Number of node points	
$P(t)$	2:6	Total power	
q, q_1	2:73		
R, r_{ij}	2:75	Matrix of order NxN	
s_i	2:55	Eigenvalues of A	
t	2:2	Time in hours	
T	4:6	Period (hrs) of the oscillations	
$u(z,t)$	2:10	Control term in buckling	
v_i	2:16	Eigenfunctions	
$X(z,t)$	2:2	Xenon concentration, measured with the xenon equilibrium concentration at infinite flux as basis	
$X^0(z)$	2:7	Equilibrium value of xenon concentration	

Contd.

Symbol	First def. in equation	Explanation	Numerical value
$\xi(z,t)$	2:7	$X(z,t) - X^0(z)$	
x	2:31, 64	State vector	
z	2:6	Space coordinate	
$\alpha(z)$	2:10	Temperature coefficient, expressed as reactivity bounded in fuel temperature increase above the moderator at mean flux and infinite gitter Normalization to mean flux $\bar{\phi}=5.65 \times 10^{13}$, $M^2=440 \text{ cm}^2$, multiply with $\frac{1}{0.0440}$	-0.226% $\alpha=-0.0514$
β	2:10	Xenon influence on changes in buckling (-3.2% on reactivity) at saturation	-0.73
γ_x	2:2	Fraction of xenon yield (relative to xenon + iodine yield)	0.05
γ_i	2:3	Fraction of iodine yield (relative to xenon + iodine yield)	0.95
$\phi(z,t)$	2:1	Neutron flux, normalized to 5.65×10^{13} neutr./cm ² sec.	
$\bar{\phi}$	2:65, 87	Mean flux	
$\phi^0(z)$	2:7	Equilibrium flux	
$\varphi(z,t)$	2:7	$\phi(z,t) - \phi^0(z)$	
λ_x	2:2	Xenon disintegration constant	0.0756 h ⁻¹
λ_i	2:2	Iodine disintegration constant	0.1058 h ⁻¹
$\lambda \text{ c}^{-1}$	2:17	Rod insertion length, rod absorbtion	
ψ	4.3.3	Form factor, $\phi_{\text{max.}} / \bar{\phi}$	
ψ_m	2:15	Eigenfunctions	
\mathcal{H}	2:51		
σ_x	2:2	Microscopic xenon cross section normalized to $\bar{\phi}=5.65 \times 10^{13}$ and time base in hours	$2.29 \times 10^{-18} \text{ cm}^2$ 0.0469
Σ_f	2:1	Macroscopic fission cross area	
Σ_a	2:1	Macroscopic absorbtion cross area	
u	2:1		
ζ	4.1.2	Measure of asymmetry	$0 \leq \zeta \leq 2$

APPENDIX 2.

PROGRAM LISTINGS

PROGRAM ASSXE

```

C
C CALCULATES THE STABILITY FOR A LINEAR TWO POINT ASYMMETRIC MODEL
C
C REF. G.OLSSON. SPATIAL XENON INSTABILITY IN THERMAL REACTORS
C DIV OF AUTOMATIC CONTROL LUND REPORT 6910
C EQ 2.52
C THE MODEL HAS FOUR STATE VARIABLES, BUT X4 IS EXCLUDED.
C THE FOURTH EIGENVALUE IS ALWAYS CONSTANT AND X4 IS INDEPENDENT
C OF THE OTHER STATE VARIABLES.
C STATE VECTOR
C X1 = XENON 1
C X2 = IODINE 1
C X3 = XENON 1 + XENON 2
C
C THE PROGRAM CAN DO TWO THINGS
C IF NP = 1
C THE CRITICAL HEIGHT IS CALCULATED FOR DIFFERENT FLUX ASYMMETRIES
C BETWEEN P AND PMIN WITH DECREMENT DP
C
C AS AN INITIAL GUESS OF CORE HEIGHT IS Z GIVEN.
C INCREMENT DZ IS ADDED FOR THE FIRST ITERATION
C MAX NUMBER OF ITERATIONS = 20
C
C EPSZ IS THE ACCURACY OF THE CRITICAL CORE HEIGHT
C
C IF NP = 2
C THE EIGENVALUES FOR A CONSTANT CORE HEIGHT ARE CALCULATED.
C ASYMMETRY IS VARIED BETWEEN P AND PMIN WITH DECREMENT DP
C
C INPUT
C Z = (CORE HEIGHT/3)**2 (IF Z LT 0 THE CALC STOPS)
C DZ = INCREMENT IN Z
C FI = MEAN FLUX
C P = ASYMMETRY MEASURE PSI, SEE SECT 4.1.2
C DP = DECREMENT IN PSI
C PM = MIN OF P
C EPSZ = ACCURACY IN CORE HEIGHT
C ALFA = TEMPERATURE COEFFICIENT
C NTES = 1 IF PRINTOUT AT EVERY ITERATION IS WANTED
C NP = 1 OR 2
C
C OUTPUT
C
C IF NP = 2
C INPUT VARIABLES, SYSTEM MATRIX
C Z, P, EIGENVALUES
C
C IF NP = 1
C INPUT VARIABLES, SYSTEM MATRIX
C Z, H(CRIT HEIGHT), P, EIGENVALUES
C MAX EIGENVALUE REAL PART AT ITERATION NO .. (IF NTES = 1)
C
C SUBROUTINE
C EIGUNS (EIGENVALUE CALCULATION, FROM PROGRAM LIBRARY)

```



```

C
C
DIMENSION A(3,3), EIGR(3), EIGI(3)
3 READ(60,100) Z,DZ,FI,P,DP,PM,EPSZ,ALFA,NTES,NP
IF (Z.LT.0.) 31,4
4 Z1 = Z
1 EG=0.0
ITE =1
2 EG1 =EG
F1 = P*FI
F2=(2.0 - P)*FI
X1 = 1.0/(1.0 +0.162/F1)
X2 = 1.0/(1.0 +0.162/F2)
XMY = 2.0/(F1*P) - Z *ALFA*2.0 +2.0/((2.0-P)*F2)
XX = -0.73 * Z * 0.469 / XMY
C
C SYSTEM MATRIX EQ 2.52 IS GENERATED
C
A(1,1) = -0.076 - 0.469*F1 + XX*(0.05-X1)
A(1,2) = 0.106
A(1,3) = -XX* (0.05 - X1)
A(2,1) = 0.95 * XX
A(2,2) = -0.106
A(2,3) = -A(2,1)
A(3,1) = -XX*(0.05-X2)
A(3,2) = -0.106
A(3,3) = -0.076 -0.469*F2 - A(3,1)
IF(ITE-1) 12,10,12
10 PRINT 200, Z,DZ,FI,P,ALFA,X1,X2,((A(I,J),J=1,3),I=1,3)
12 CONTINUE
C
C EIGENVALUES ARE CALCULATED
C
CALL EIGUNS (A,EIGR,EIGI,3,3,IP,IER)
IF (NP.EQ.2) 150,30
30 CONTINUE
IK0 = IER + 1
GOTO (40,32,33) IK0
32 PRINT 1001
GOTO 91
33 PRINT 1002
GOTO 91
40 CONTINUE
C
C CALCULTAION OF THE REAL PART OF THE BIGGEST EIGENVALUE
C ITERATION OF CORE HEIGHT UNTIL THE BIGGEST EIGENVALUE IS ZERO
C THEN THE CRITICAL HEIGHT IS REACHED
C
EG = EIGR (1)
DO 38 I38 = 1,2
IF (EG - EIGR(I38 + 1)) 35,35,38
35 EG = EIGR(I38+1)
38 CONTINUE
IF (NTES.EQ.1) 36,37
36 PRINT 1020, EG,ITE,Z,P
37 IF (ABS(EG).LE.1.0E-4) 90,41

```

```

41     ITE = ITE + 1
      IF(ITE - 20 ) 51,51,90
51     IF(ITE-2) 55,53,55
53     Z = Z+DZ
      GOTO 2
55     EG2 = EG - EG1
      IF(ABS(EG2).LE.1.0E-4) 90,57
57     DDZ=(Z1-Z)*EG/EG2
      IF(ABS(DDZ).LE.EPSZ) 90,59
59     Z1 = Z
      Z = Z+DDZ
      IF(Z.GT.100.0) 99,2
C
C     THE CRITICAL HEIGHT IS REACHED
C     THE HEIGHT AND EIGENVALUES ARE PRINTED OUT
C
90     ZH=SQRT(Z)*3.0
      PRINT 1010,Z,ZH,P,(EIGR(I),EIGI(I),I=1,3)
91     P = P - DP
      IF(P.LT.PM) 99,1
99     GOTO 3
31     PRINT 220
      CALL EXIT
150    PRINT 1040, Z,P, (EIGR(I),EIGI(I),I=1,3)
      P = P - DP
      IF (P.LT.PM) 99,1
100    FORMAT (7F5.0,F10.0,2I1)
200    FORMAT (10X,2HZ=,F10.4,5H DZ=, F10.4,6H FIM=,F8.4,6H PSI=,
1 F8.4, 7H ALFA=, F10.6, 8H XENON=, 2F10.5/10X,10HMATRISEN A/
2 (20X,3F12.6/))
220    FORMAT (10X,3HEND)
1001   FORMAT (25H TRIDIAGONALISATION FAILS )
1002   FORMAT (23H MULLER ITERATION FAILS )
1010   FORMAT (10X,2HZ=,F10.4,4H H=, F10.4, 6H PSI=,F10.5/10X,
16HEIGENV,2F10.6/15X,2F10.6/15X,2F10.6)
1020   FORMAT (/10X,24HMAX EIGENVALUE REAL PART, F15.7,3X, 9HITERATION
1 ,2X,2HN0,I4,2X,3HH2=, F8.4, 2X,2HP=, F10.6)
1040   FORMAT (10X,2HZ=, F10.4, 6H PSI=, F10.4/ 10X,6HEIGENV/
1 (15X,2F10.6/))
      END

```

PROGRAM XELT

C
 C CALCULATES THE CRITICAL HEIGHT FOR A LINEAR AXIAL MODEL OF
 C A REACTOR.
 C THE FLUX SHAPE IS EITHER FLAT OR SINUSODIAL (WITH CONST BUCKLING)
 C
 C THE NUMBER OF MESHPOINTS IS VARIED BETWEEN N AND NMAX (LT 20)
 C
 C AS AN INITIAL GUESS OF CORE HEIGHT IS H GIVEN.
 C DH IS THE VARIATION OF H AT FIRST ITERATION.
 C HMAX IS A MAXIMUM VALUE OF H WHICH MUST NOT BE EXCEEDED DURING
 C THE ITERATIONS

C REF. G. OLSSON. SPATIAL XENON INSTABILITY IN THERMAL REACTORS
 C DIV OF AUTOMATIC CONTROL LUND REPORT 5910
 C ED 2.57-59
 C FLAT FLUX 2.66
 C SINE FLUX 2.85

INPUT

C FTM = MEAN FLUX (IF FTM LT 0 THE CALCULATION STOPS)
 C H = INITIAL GUESS OF CORE HEIGHT
 C DH = FIRST ITERATION OF CORE HEIGHT
 C HMAX = MAX CORE HEIGHT
 C EPSH = ACCURACY IN DETERMINATION OF CRITICAL CORE HEIGHT
 C ALFA = TEMP. COEFF.
 C N = NUMBER OF SPACE POINTS. (LT 20)
 C NMAX = MAX NUMBER OF SPACE POINTS IN THE CALCULATION
 C ITEM = MAX NUMBER OF ITERATIONS
 C IP = 1 IF PRINTOUTS OF TEST VALUES FROM SUBROUTINE ETGUNS IS WANTED
 C 0 ELSE
 C NTES = 1 IF BIGGEST EIGENVALUE AT EVERY ITERATION SHALL BE PRINTED
 C IFLUX = 1 FOR FLAT FLUX AND = 2 FOR SINUSODIAL FLUX (CONST. BUCKLING)

OUTPUT

C STABILITY LIMIT H=
 C EIGENVALUES REAL AND IMAG. PART
 C
 C IF NTES = 1
 C MAX EIGENVALUE REAL PART = . . . ITERATION NO . . .
 C H = . . . N = . . .
 C IF IP = 1
 C TESTVALUES OF SUBROUTINE ETGUNS

SUBROUTINES

C FLUX
 C GJRY (MATRIX INVERSTION FROM PROGRAM LIBRARY)
 C ETGUNS (EIGENVALUE CALCULATION FROM PROGRAM LIBRARY)

C DIMENSION A(20*20),ETGR(20),ETGT(20)
 C COMMON H2,ALFA,FTM,N,G(20*20),F1(20),XN(20),XNM,IFLUX
 2000 READ(60,100) FTM,H,DH,HMAX,EPSH,ALFA,N,NMAX,ITEM,IP,NTES,IFLUX
 IF(FTM.LE.0.0)2003,2001

```

2001 PRINT 200, FIM,H,DH,HMAX,EP SH,ALFA,N,NMAX,ITEM,IP,NTES,IFLUX
      HI = H
1     EG = 0.0
      ITE = 1
2     EGI = EG
      HH = H/(FLOAT(N+1))
      H2 = HH * HH
      DO 10 K = 1,N
      DO 12 KK = 1,N
      G(K, KK) = 0.0
12    CONTINUE
10    CONTINUE
      N2 = 2 * N
      NM1 = N - 1
      N2M = 2 * N - 2
      N2M1 = 2*N - 1
      DO 13 I13 = 1,N2
      DO 14 I14 = 1,N2
      A(I13,I14) = 0.0
14    CONTINUE
13    CONTINUE
C
C     IN SUBROUTINE FLUX IS CALCULATED THE MATRIX G OF EQ. 2.73
C
C     CALL FLUX
C
C     INVERSION OF THE G MATRIX
C
      GOTO (15,16) IFLUX
15    CALL GJRV(G,NM1,1.0E-8,TERR,20)
      GOTO 17
16    CALL GJRV(G,N,1.0E-8,TERR,20)
17    IF (TERR.EQ.(-1)) 18,19
18    PRINT 1005, N
      GOTO 91
C
C     GENERATION OF FLUX VECTOR AND SYSTEM MATRIX A OF THE XENON PROC
C     EQ 2.57-58
C
19    D = 0.34237 * H2
      JF(IFLUX,EO,2) 70,24
24    DO 25 I25 = 1,N
      DO 30 J30 = 1,N
      D2 = G(I25,J30) * FI(J30) * D
      A(2*I25-1, 2*J30-1) = D2 *(XN(I25)-0.05)
30    A(2*I25, 2*J30-1) = -0.95 *D2
      A(2*I25-1, 2*I25-1) = A(2*I25-1,2*I25-1) -0.076 -0.469*FI(I25)
      A(2*(I25-1),2*I25) = 0.106
25    A(2*I25, 2*I25) = -0.106
      GOTO 20
70    DO 72 I72 = 1,N
      GSUM = 0.0
      DO 74 J74 = 2,N
      D2 = G(I72,J74) * FI(J74) * D
      A(2*I72-1, 2*J74-1) = D2 * (XN(I72) - 0.05)
      GSUM = GSUM + G(I72, J74) * FI(J74)

```

```

74      A(2*172, 2*172-1) = -0.95 * D2
      DGS = -D * GSUM
      A(2 * 172 - 1, 1) = DGS * (XN(172) - 0.05)
      A(2*172,1) = -DGS * 0.45
      A(2*172-1, 2 * 172 - 1) = A(2*172-1, 2*172-1) - 0.076 = 0.469*
1      FI(172)
      A(2*172 - 1, 2*172) = 0.106
72      A(2 * 172, 2 * 172) = -0.106
20      GOTO (26,27) IF LUX
C
C      CALCULATION OF EIGENVALUES
C
26      CALL EIGONS (A, EIGR, EIGI, N2M, 20, IP, IER)
      GOTO 28
27      CALL EIGONS (A, EIGR, EIGI, N2, *20, IP, IER)
28      IRO = IER + 1
      GOTO (40,32,33) IRO
32      PPINT 1001
      GOTO 91
33      PRINT 1002
      GOTO 91
C
C      CALCULATION OF THE REAL PART OF THE BIGGEST EIGENVALUE
C      ITERATION OF THE CORE HEIGHT UNTIL THE BIGGEST EIGENVALUE IS ZERO
C      THEN THE CRITICAL HEIGHT IS REACHED
C
40      IF (IFLUX, EQ, 1) 50,61
50      EIGR(N2M1) = -0.076 - 0.469 * FIM
      EIGI (N2M1) = 0.0
      EIGR (N2) = -0.106
      EIGI (N2) = 0.0
61      EG = EIGR (1)
      DO 38, I38 = 1, N2M
      IF (EG - EIGR(I38 + 1)) 35,35,33
35      EG = EIGR(I38+1)
38      CONTINUE
      IF (NTE5, EQ, 1) 30,37
36      PRINT 1020, EG, ITE, H, M
37      IF (ABS(EG), LE, 1.0E-4) 90,41
41      ITE = ITE + 1
      IF (ITE - ITEM) 51,51,40
51      IF (ITE-2) 55,53,55
53      H = H + DM
      GOTO 2
55      EG2 = EG - E01
      IF (ABS(EG2), LE, 1.0E-4) 90,57
57      DDH = (H1-H)*EG/EG2
      IF (ABS(DDH), LE, EPSH) 90,59
59      HT = H
      H = H + DDH
      GOTO 2
C
C      THE CRITICAL HEIGHT H IS CALCULATED AND THE EIGENVALUES ARE PRINTED
C
90      PRINT 1010, H, M
      PRINT (0)

```

```

      DO 93 I93 = 1, N2
93    PRINT 1012, EIGR(I93), F16I(I93)
94    N = N+1
      IF (N.GT.999) 99,1
99    GOTO 2000
2003  PRINT 210
      CALL EXIT
100   FORMAT (4F5.0,2F10.0,6I2)
200   FORMAT (10X,3HF)=,F8.3,2X,2HH=,F8.3,2X,3HH=,F8.3,2X,5HHMAX=,
1    F8.3,2X,5HEPSH=,F8.3,2X,5HALFA=,F9.5/4X,
2    2X,2HN=,13,2X,5HHMAX=,13,2X,5HITEM=,13,
3    2X,3HIP=,13,2X,5HMIES=,12,3X,6HFLUX=,13)
210   FORMAT (10X,3HEND)
1001  FORMAT (25H TRIDAGONALISATION FAILS )
1002  FORMAT (23H MULLER ITERATION FAILS )
1005  FORMAT (5X,19H INVERSION FAILED N=,I2)
1010  FORMAT (7775X,18H STABILITY LIMIT H=,F10.4,3H M,15X,2HN=,13//)
1011  FORMAT (10X,11HE EIGENVALUES,2X,4HREAL,12X,4HMAG)
1012  FORMAT (20X,2F16.5)
1020  FORMAT (/10X,24HMAX EIGENVALUE REAL PART, F15.7,3X,9H ITERATION
1    ,2X,2HN=,14,2X,2HH=,F8.4,2X,2HN=,I2)
      END

```

```

SUBROUTINE FLUX
C
C CALCULATES THE G MATRIX OF FLAT AND SINE FLUX
C
C REF. G. OLSSON. SPATIAL XENON INSTABILITY IN THERMAL REACTORS
C DIV OF AUTOMATIC CONTROL LUND REPORT 6910
C FO 2.73 FLAT FLUX
C FO 2.86 SINE FLUX
C
COMMON HZ,ALFA,F (9*N,6(20,20),F1(20),XN(20),XNM,IFLUX
NM1 = N-1
NM2 = N-2
GOTO (1,2) IFLUX
C
C FLAT FLUX
C
1 CONTINUE
DO 15 I15 = 1,N
15 FI(I15) = FIM
G1 = 1.0 - HZ * ALFA * FIM
G6 = 1.0 + G1
XNM = 1.9 / (1.7 + 0.162 / FIM)
DO 17 I17 = 1,N
17 XG(I17) = XNM
IF(N,50,2) 20,21
20 G(1,1) = G6
GOTO 1000
21 DO 25 I25 = 2,NM1
25 G(I25,I25) = G6
G(I,1) = G1
G(N-1,N-1) = G(N-1,N-1) + 1.0
29 DO 30 I30 = 2,NM1
30 G(I30-1,I30) = -1.0
30 G(I30,I30-1) = -1.0
DO 35 I35 = 1,NM2
35 G(N-1,I35) = 1.0
G(N-1,N-2) = 0.0
GOTO 1000
C
C SINE FLUX HOMOGENEOUS CONTROL
C GENERATION OF STATIONARY FLUX FO 2.82
C
2 CONTINUE
46 SN = 1.0 / (FLOAT(N+1))
S = 2.0 * COS(3.1415927 * SN)
F1(1) = 1.0
F1(2) = S
DO 50 I50 = 2,NM1
50 F1(I50+1) = S * F1(I50) + F1(I50-1)
SUM = 0.0
DO 52 I52 = 1,N
52 SUM = SUM + F1(I52)
C
C FLUX IS NORMED TO MEAN FLUX FIM
C STATIONARY XENON VALUES ARE CALCULATED

```

```

C
      P = SUM*SN
      PI = F[14/P
      DO 55 I55 = 1,N
      FI(I55) = P]*FI(I55)
55      XN(I55) = 1.0/(1.0+0.162/FI(I55))
C
C      GENERATION OF THE G MATRIX 2*36 WITH THE CONDITION 2*60 TO ELIMINATE C
C
      DO 60 I60 = 1,N
60      G(I60*160) = S - H2*ALFA*FI(I60)
      DO 62 I62 = 1,NMI
      G(I62*162 + 1) = -1.0
62      G(I62+1*162) = -1.0
      DO 64 I64 = 2,N
      G(I64*1) = G(I64*1) - FI(I64) * G(1*1) / FI(1)
64      G(I64*2) = G(I64*2) + FI(I64) / FI(1)
      DO 66 I66 = 1,N
66      G(1*I66) = 1.0
1000  RETURN
      END

```


PROGRAM XETRA

```

C
C THE PROGRAM CALCULATES A XENON TRANSIENT OUT OF A TWO POINT NONLINEAR
C SYMMETRIC MODEL
C THE CONTROL CAN BE A ROD OR HOMOGENEOUS CONTROL
C THE ROD IS ACTING IN POINT 1
C
C
C INPUTS
C FI = MEAN FLUX          TMAX = INTEGRATION TIME IN HOURS
C DT = TIME STEP IN HOURS      H2 = (HEIGHT/3)**2
C X = STATE VECTOR        X1 = XENON1          X3 = IODINE 1
C                          X2 = XE1 + XE2      X4 = IODINE1 + IODINE2
C XMAX = PERMITTED MAX FOR THE STATE VECTOR
C REV = 1.0 FOR POSITIVE TIME AND = -1.0 FOR NEGATIVE TIME
C ALF = TEMP. COEFF.      MC = 1 FOR HOM. CONTROL AND = 2 FOR ROD CONTROL
C NTRY = NUMBER OF TIME STEPS BETWEEN PRINTOUTS
C
C
C OUTPUT
C DFI = DEVIATION OF FLUX IN POINT ONE
C TIME, X1, X2, X3, X4, DFI
C
C SUBROUTINE REQUIRED
C RK1ST (A RUNGE-KUTTA ROUTINE FROM THE PROGRAM LIBRARY)
C FUNC
C
C
C REF. G. OLSSON. SPATIAL XENON INSTABILITY IN THERMAL REACTORS
C DIV OF AUTOMATIC CONTROL LUND REPORT 6910
C EQ. 2.37-40
C
COMMON /FLUX/ DFI, G, H2, XN, ALF, FI, REV, MC
DIMENSION DX(4), XE(10), X(10), XMAX(4)
1 READ (60,101) FI, TMAX, DT, H2, (X(I), I=1,4), (XMAX(I), I=1,4), REV, ALF
1 MC, NTRY
II = NTRY
IF(FI) 80,80,3
3 WRITE(61,102) FI, TMAX, DT, H2, (X(I), I=1,4), (XMAX(I), I=1,4), REV, ALF
1 MC
DFI = 0.0
T = 0.0
XN = 1.0 / (1.0 + (0.162/FI))
G = 2.0/H2 - ALF*FI
DO 6 I6 = 1,4
XE(I6) = X(I6)
6 CONTINUE
WRITE (61,103) XN, G
8 CALL RK1ST (T, X, DT, XE, 4, 10)
II = II - 1
IF(II) 51,50,51
50 WRITE (61,110) T, (X(K), K = 1,4), DFI
II = NTRY
51 DO 14 K = 1,4

```

```
DX(K) = ABS(X(K)) - XMAX(K)
IF(DX(K)) 14,14,70
14 CONTINUE
18 IF(TMAX - T) 70,22,22
22 T = T + DT
DO 10 I10 = 1,4
X(I10) = XE(I10)
10 CONTINUE
GOTO 8
70 GOTO 1
80 WRITE (61,115)
101 FORMAT (4F5.0,4F10.0/5F5.0,F10.0,2I2)
102 FORMAT (10X,3HF1=, F8.4,2X,5HTMAX=, F8.4,2X,3HDT=,F8.4,2X,
1 3HH2=,F8.4,2X,3HX0=,4F8.4 /10X,5HXMAX=,4F8.4,
2 2X,3HREV,F5.2, 2X, 5HALFA=, F10.5, 10H CONTROL, I2)
103 FORMAT (10X, 6HXENON=, F8.4, 2X, 2HG=, F8.4//13X,4HTIME,
1 10X,2HX1,10X,2HX2,10X,2HX3,10X,2HX4,10X,3HDFI)
110 FORMAT (10X, F8.3, 5F12.5)
115 FORMAT (10X,3HEND)
CALL EXIT
END
```

SUBROUTINE FUNC

```

C
C   FUNC DEFINES THE RIGHT HAND SIDE OF THE DYNAMICAL SYSTEM OF THE
C   TWO POINT NONLINEAR XENON MODEL
C
C   REF.   G.O.LSSON.   SPATIAL XENON INSTABILITY IN THERMAL REACTORS
C           EQ.   2.37-40
C
C           DIMENSION DXDT(10), Z(10)
C           COMMON/FUNCTION/ T,Z,DXDT
C           COMMON /FLUX/ DFI,G,H2,XN,ALF, FI,REV,MC
C           R = G + 0.73*(Z(2) - Z(1))
C           IF(MC.EQ.2) 2,1
C
C   DFI FOR HOMOGENEOUS CONTROL IS CALCULATED   EQ. 2.46
C
C   1   IF (ABS(ALF).LE.1.0E-4) 3,4
C
C   THE CASE ALFA = 0   EQ. 2.47
C
C   3   IF (ABS(2.0*Z(1) - Z(2)).LE.1.0E-5) 20,22
C   20  DFI = 0.0
C       GOTO 8
C   22  GG = -FI*G*1.3699 / (2.0*Z(1) - Z(2))
C       DFI = -GG + SQRT(GG*GG + FI*FI)
C       GOTO 8
C
C   THE CASE ALFA NOT EQUAL TO ZERO   EQ. 2.46   THE EQ. IS GENERATED
C
C   4   DFI = DFI
C       DF2 = DFI
C       A1 = -0.365 * (2.0 *Z(1) - Z(2))/ALF
C       B1 = G * FI / ALF
C       C1 = 0.365 * (2.0*Z(1) - Z(2)) * FI*FI/ALF
C   26  DFI = DF2
C       FI2 = DFI*DFI
C       FI3 = FI2 * DFI
C
C   THE EQ. 2.46 IS SOLVED WITH NEWTON-RAPHSON
C
C       DF2 = (2.0*FI3 + A1*FI2 - C1)/(3.0*FI2 + 2.0 *A1*DFI + B1)
C       IF (ABS(DF2-DFI).LE.1.0E-8) 24,26
C   24  DFI = DF2
C       GOTO 8
C
C   DFI IS CALCULATED FOR ROD CONTROL   EQ.2.42
C   THE ROD IS ACTING IN POINT 1
C
C   2   IF (ABS(ALF).LE.1.0E-4) 5,7
C   5   DFI = FI/(1.0 + (1.3698*G)/(Z(2) - Z(1)))
C       GOTO 8
C   7   CONTINUE
C       DFI = -(B/(2.0*ALF)) * (1.0-SQRT(1.0+2.92*ALF*FI*(Z(2)-7(1))
C   1 )))
C   8   CONTINUE

```

C
C
C

THE RIGHT HAND SIDE OF EQ 2.37-40 IS CALCULATED

1 DXDT(1) =REV*((-0.076-0.469*FI)*Z(1)+0.106*Z(3)+(0.02345-0.469
1 *(XN+Z(1)))*DFI)1 DXDT(2) =REV*((-0.076-0.469*FI)*Z(2)+0.106*Z(4)+(0.469*Z(2)
1 -0.938*Z(1))*DFI)

DXDT(3) = REV* (-0.106*Z(3) + 0.44555 *DFI)

DXDT(4) = REV*(-0.106*Z(4))

12

RETURN

END